Department of Mechanical and Aerospace Engineering

Investigation of Harmonic Phenomena in a Tidal Power System

Author: Maria-Faidra Katsiantoni

Supervisor: Olimpo Anaya-Lara

A thesis submitted in partial fulfilment for the requirement of the degree

Master of Science

Sustainable Engineering: Renewable Energy Systems and the Environment

2012

Copyright Declaration

This thesis is the result of the author's original research. It has been composed by the author and has not been previously submitted for examination which has led to the award of a degree.

The copyright of this thesis belongs to the author under the terms of the United Kingdom Copyright Acts as qualified by University of Strathclyde Regulation 3.50. Due acknowledgement must always be made of the use of any material contained in, or derived from, this thesis.

Signed: Maria-Faidra Katsiantoni   Date:

6/09/2012

Acknowledgements

Abstract

The aim of this thesis is the conduction of a sensitivity analysis for the investigation of causes of voltage harmonics in a tidal power system. The examined system comprises of a squirrel cage induction generator connected to a subsea cable through a step down transformer which leads to a back to back voltage source converter and is connected to the grid through a step-up transformer.

The above mentioned power system was modelled in Simulink SimPowerSystems. System components that were parameterised for the sensitivity analysis include the subsea cable's length and the transformer's magnetising inductance. A harmonic filter was also applied at the Low Voltage side of the transformer and it was tuned to different resonant frequencies as a part of this analysis. The procedure that was followed for the conduction of this analysis was used as a basis for the development of a methodology for the prevention of system resonances and the mitigation of harmonics though the design of passive filters. As an attempt to automate this methodology in Simulink, a script with Matlab code was also developed for the masking of different parameters and the collective acquisition of results for comparison.

System elements that were parameterised include:

- The subsea cable length and number of PI sections

- The transformer's magnetising inductance

- The output reactor's inductance

- The harmonic filter's resonant frequency

The simulations that were run indicated that changes in the system inductances can cause resonances, hence significant distortion in the waveforms. Additionally, it was observed that tuning the filter away from the converter's switching frequency causes an elevation in the percentage of total harmonic distortion by 2% on average.

Contents

List of figures

List of Tables

Nomenclature

AC-Alternating Current

BPF-Bandpass filter

BSF-Bandstop filter

C-Capacitance

Cnes-Centre Nationale d' Etudes

Spatiales

DC-Direct Current

DCT-Direct Torque Control

DFIG-Doubly Fed Induction

DNO-Distribution Network Operator

EMEC-European Marine Energy

Centre

E.M.F.-Electromagnetic field

EMI-Electromagnetic Interference

f-Frequency

FRC-Full Rated Converter

FSIG-Fixed Speed Induction

Generator

h-Harmonic order

HV-High Voltage

I-Current

IEC-International Electrotechnical

Commission

IGBT- Insulated-Gate Bipolar

Transistor

KW-Kilowatt

L-Inductance

LPF-Lowpass filter

LV-Low Voltage

m-Modulation factor

P-Power

PCC-Point of Common Coupling

(S)PWM-(Sinusoidal)   Pulse   Width

Modulation

R-Resistance

T-Torque

THD-Total Harmonic Distortion

V-Voltage

VFD-Variable Frequency Drive

VSC-Voltage Source Converter

X-Reactance

Z-Impedance

α-Transformation ratio

φ-Phase angle

ω-Radial frequency

1 Introduction

The constantly increasing demand for emission free energy imposes the development of renewable power systems. Offshore developments, and especially tidal, seem particularly attractive due to the minimal disturbances on the site and the predictability of the tidal cycles (EMEC, 2012). Due to the low flow speeds in tidal streams tidal turbines generate electricity with low frequency, thus, a frequency converter will be required onshore in order to provide power at the grid frequency.

Non-linear switching devices, such as a frequency converter, are the main source of harmonics in power systems (Amin, 1997). Other identified harmonic sources are non-linear magnetic elements (e.g. saturated transformer cores) and non-sinusoidal air gap flux distribution in rotating AC machines (Acha, et al., 2002). Harmonic voltages and currents have major effects to power quality as well as rotating machinery (IEEE STANDARDS, 1993). A common consequence in generators and motors is increased heating due to iron and copper losses at harmonic frequencies which influences the machine's efficiency and torque. Other implications caused by harmonic distortion include interference to communication systems for controls and data acquisition and to any type of electronic circuit, as well as electrical and electromechanical resonance that can respectively cause over-voltages/over-currents and vibration and therefore mechanical part fatigue failure (Acha, et al., 2002). In an offshore tidal power system a combination of component parameters can cause resonances and increase the harmonic content in the machine side as well as in the grid side.

The most common way to combat voltage and current harmonics is the introduction of suitable passive filters, which can also contribute to reactive power compensation, usually in the Low Voltage side of the system, for economic reasons.

Identifying the causes of harmonics and resonances and coming up with effective mitigation measures has always been a challenge in power systems (Daniel J. Carnovale, et al., 2003).

The purpose of this thesis is to investigate in what ways the power quality, and hence the harmonic content, in a tidal system is affected by changes in system impedances

as well as to what extend it is affected and whether any system resonances are likely to occur. Moreover, this project aims to examine the application of a passive filter for the mitigation of harmonics and, finally, propose a methodology that can be followed for the identification of sources of harmonics and the filter design in a generic tidal system.

After simulations were run and the results were assessed it was observed that in the machine side of the system significant harmonic distortion occurs in frequency sidebands near the frequency converter's switching frequency, thus, a passive filter tuned in this frequency could lead to acceptable voltage and current waveforms. It was also concluded that in a system relatively close to shore (distance from shore less than 20km) the cable length does not have significant influence on the system in terms of harmonic content.

The first part of the thesis presents a literature survey on tidal energy, as well as the system components, the sources of harmonics along with their consequences and the ways that they can be mitigated, with more attention being drawn to passive filters. Following the literature survey, the examined Simulink model is presented and analysed and equations that lead to sizing of the system are derived. The third part refers to the simulations that were carried out and their results; the parameters that were varied are presented along with the way that the results were assessed. Discussion about the findings is also included. A concluded methodology is then provided for the prevention and mitigation of harmonic phenomena and the design of suitable passive filters in a resembling system. Finally, the conclusions that were reached after the conduction of this investigation are summarised and recommendations for future work are also provided, for an enhanced system representation and assessment of results. Within the Appendices section of this thesis more detailed results are provided and also a commented matlab script that can be used and further developed in future work for the automation of the resulting methodology and for running unattended simulations.

2 Literature review

2.1 Tidal Energy

Tidal streams and currents are generated by the relative move of the earth the sun and the moon (Sheth & Shahidehpour, 2005). More specifically, the gravitational forces between the sun and the moon and earth's waters and they generate 2 type of tides in the oceans; neap and spring tides (Strathclyde, 2005).
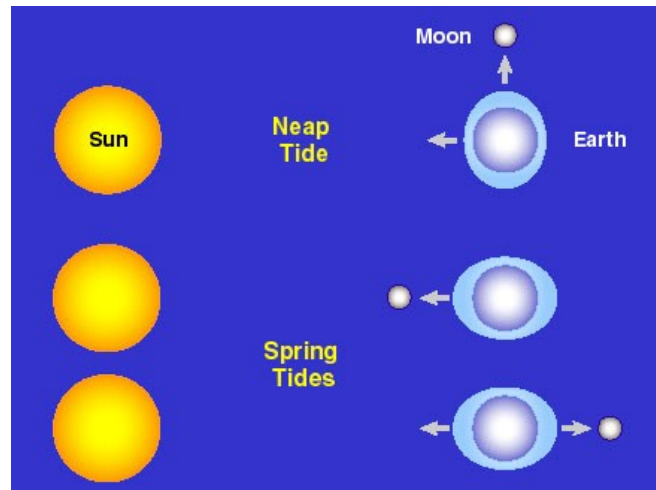
Figure 2.1Tidal cycle Source: (Strathclyde, 2005)

This phenomenon is exploited for the generation of renewable energy coming from marine currents and tidal streams. While during the 1990's research related to tidal energy focused on tidal barrages, which take advantage of tidal elevation, due to their high power density and efficiency, their limitation imposed by high capital costs and considerable environmental impact lead research to focus on tidal stream energy using tidal current mills *(Charlier, 2003).*The main benefits in tidal stream energy installations as compared to offshore wind farms include predictability, high power density, absence of extreme flow speeds and minimal audio and visual disturbance *(Blunden & Bahaj, 2006)* as well as disturbance in marine traffic. However, tidal energy tends to be more site-specific as demonstrated in figure 2.2.
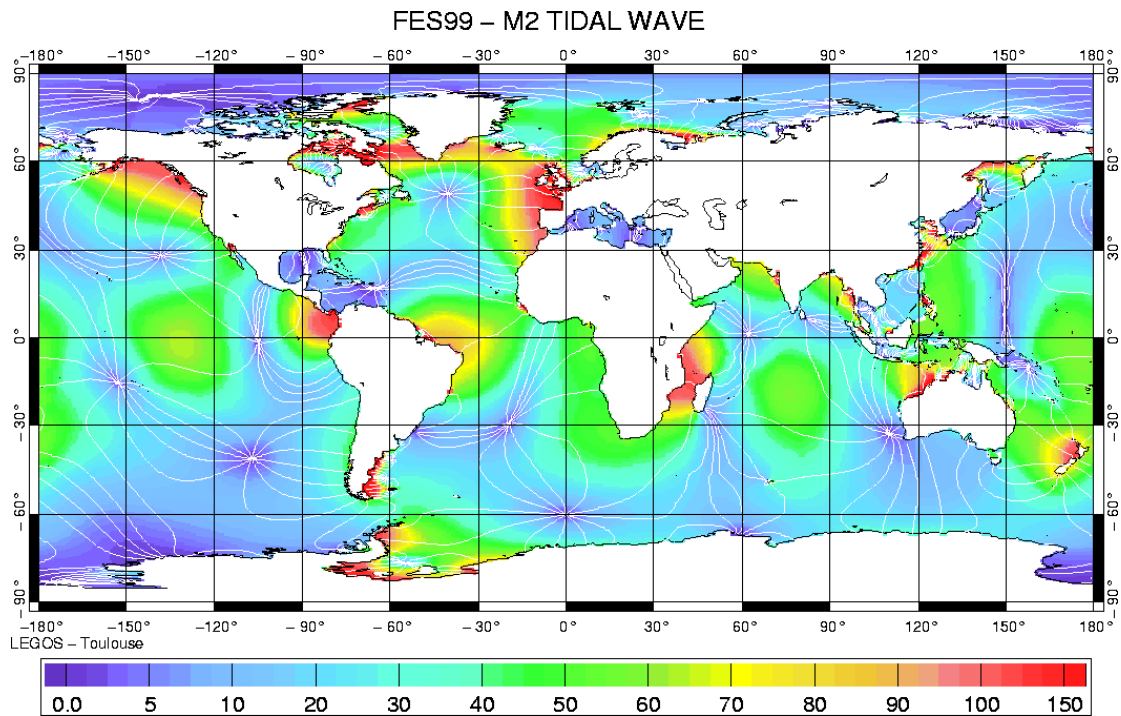
Figure 2.2 Map of tidal potential worldwide. Source: (Cnes, 2000)

A 'typical' configuration for a tidal power system does not exist as they are still under research and there are no tidal systems commercially deployed yet. However, it would be safe to say that it would resemble the configuration of an offshore wind power system, with changes depending on the distance from shore. Thus, a generic system that can provide an insight at the system which will be studied in the next chapters can be seen in figure 2.3; a short literature review for each one of the components presented in figure 2.3 is provided in the upcoming units.
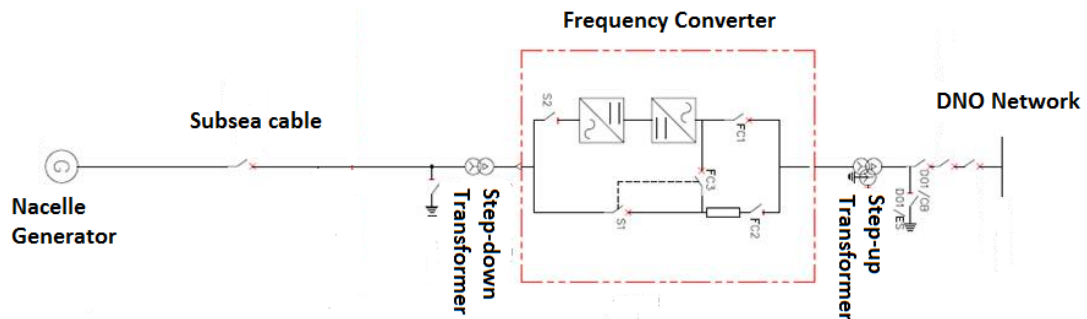
Figure 2.3 Generic Tidal System

As illustrated in figure 2.3 the system consists of the generator which is in the nacelle, and it connected to the shore through a subsea cable. On shore, a frequency converter is needed to convert low frequency power coming from the tidal generator (which operates in low flow speeds) to power that will comply with grid regulations (50Hz) and will not cause any disturbances. Whether one or more transformers are required or not, depends on a number of factors such as the operating voltage of the generator,

the manner of power transmission to shore (AC, HVDC), the operating voltage of the frequency converter and the voltage level at the point of common coupling (PCC). Although the existence of transformers would raise the installation's cost and increase the losses, the additional inductance provided by it would be beneficial for the voltage and current waveforms on distortion terms.

2.2   Squirrel cage generator

The squirrel cage induction generator shows extreme simplicity and ruggedness; which, along with its low cost and minimal maintenance requirements makes it one of the most commonly used type of machine (Fitzgerald, et al., 2003). Especially in renewable energy industry,

Figure 2.4 Squirrel cage induction machine (Harmonic Media, 2012)

asynchronous generators are preferred as their speed varies according to the turning force applied to them, causing less wear and tear at the gearbox while enhancing energy capture at the same time with simple control methods (Chapman, 2000).

Tidal power systems are not commercially developed yet, hence there is no fixed preferred configuration of such a system (i.e. no collective conclusions on the types of generators used, the point of energy conversion, the manner of connection to shore etc.). Although in most offshore wind power systems a variable speed generator is considered most suitable (e.g. DFIG or FRC) (Böhmeke, et al., 1997), in a respective tidal system a fixed-speed generator (FSIG) such as a squirrel cage induction generator would seem as a more

Figure 2.5 Comparison of a fixed speed (a) and variable speed (b) wind turbine system. Source: (Anaya-Lara, et al., 2009)

reasonable choice. This is justified considering that in a variable speed system the rotor winding would need to be fed through a variable frequency converter for the decoupling of the mechanical from the electrical grid frequency, while in the case of a fixed speed system where the speed variations are insignificant this would not be required (Anaya-Lara, et al., 2009). Thus, the presence of a power electronic topology underwater in the turbine hub would not be preferable as it would add complexity and reliability issues, require more sophisticated controls.

2.3 Power Electronics operation.

Power electronic systems have been developed radically during the last decades due to the growth of renewable energy industry; they are merely switching devices that control current to provide variable speed and frequency output (Fitzgerald, et al., 2003). In the examined application a power electronic topology is required to convert

variable frequency power from a tidal turbine into constant frequency power that can be fed to the grid. The main components of a power electronic converter include the power circuit that consists of switches and passive elements (resistances, inductances etc.) and a control and protection system that dictates the converter's output; the link between those parts includes gating and feedback control signals (Yazdani & Iravani, 2010).

A short reference is made to the different types of composite (AC-DC-AC) converters. The two main categories of converters for variable frequency drives (VFDs) are those for current source inverter drives (CSI) and those for voltage source inverter drives (VSI) (Bose & van Wyk, 1997), whose topologies are shown in figures 2.6 and 2.7 respectively. Both types of VFDs consist of a converter, a DC link and an inverter. A CSI uses SCRs and GCTs in the converter section, while the DC link has inductors for the current's ripple regulation and the inverter uses either GTO or SGCT switches for the implementation of the PWM. A VSI, on the other hand, uses a diode rectifier as a converter, its DC link consists of parallel capacitors and the inverter typically comprises IGBT switches (Bose, 2006) (Wu, 2006)
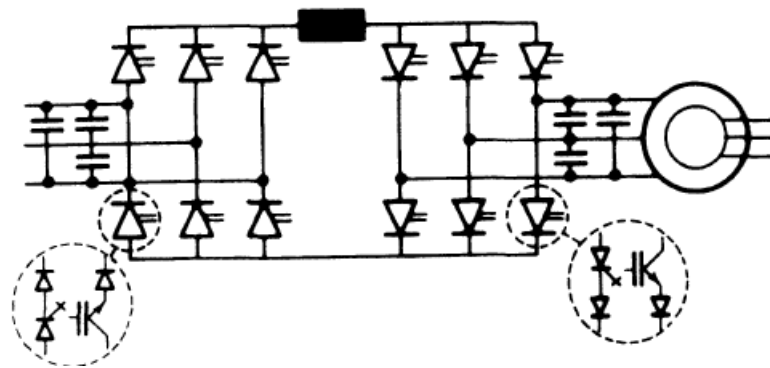
Figure 2.6 Current mode PWM rectifier feeding a current-sourced PWM inverter.

Source: (Bose & van Wyk, 1997)
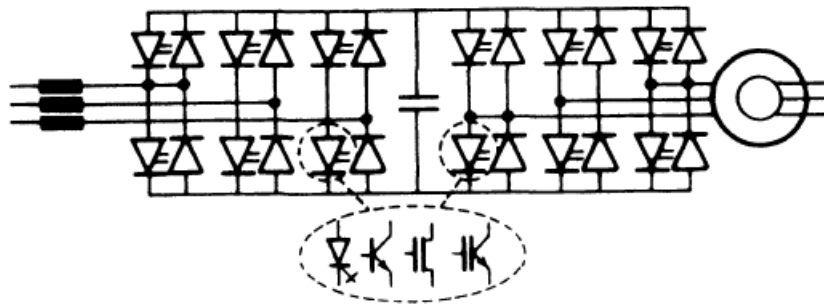
Figure 2.7 Three phase PWM rectifier feeding voltage-sourced PWM inverter. Source: (Bose & van Wyk, 1997)

The converter that is included in this thesis's examined system is a two level Voltage-Source converter. It consists of two voltage source inverter bridges that are connected back to back; the network side bridges insures fixed frequency fed to the grid whereas the machine side bridge provides variable frequency and voltage control to the squirrel cage induction generator (Jones & Smith, 1993).

The method of control implemented is termed as encoderless flux vector control, also known as Direct Torque Control (DCT). In this type of control does not require a shaft-mounted incremental encoder for the acquisition of the shaft speed that would affect the system's robustness (B.P.Conroy, et al., 1995). The converter's output voltage is dictated and applied to the machine through a look-up table so that constant flux is insured and the torque is controlled through the stator's flux speed (Zaimeddine & Undeland, 2010).

Figure 2.8 demonstrates the block diagram of the machine side of the system, where a voltage source converter controls an asynchronous machine.
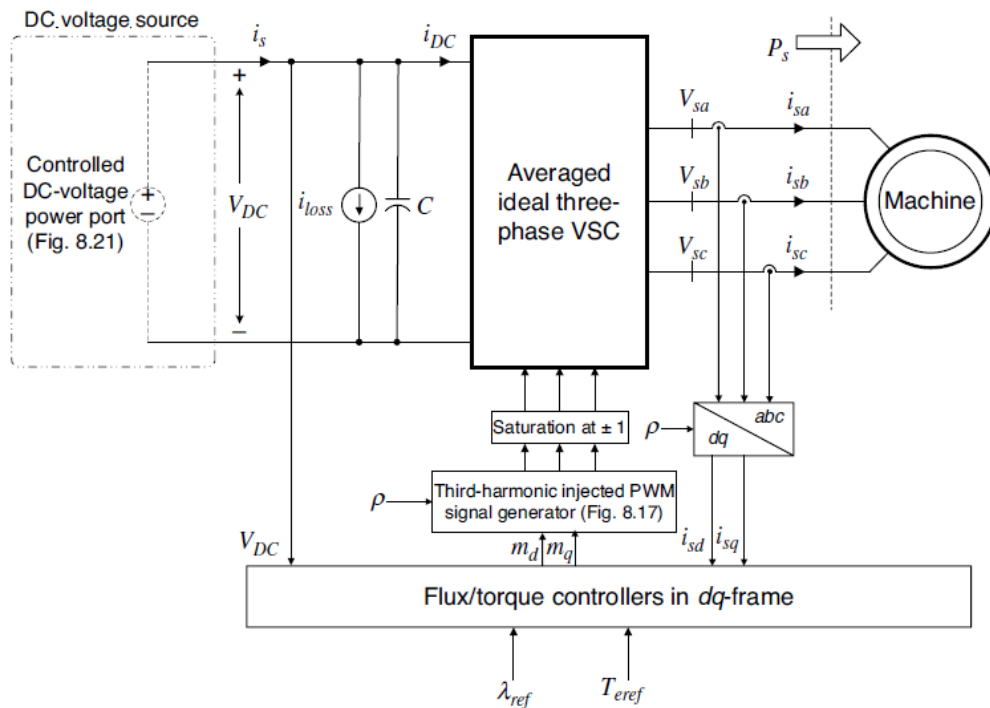
Figure 2.8 Variable frequency voltage source converter that controls an asynchronous machine. Source: (Yazdani & Iravani, 2010)

2.4   Pulse Width Modulation Method (PWM)

According to (Mohan, et al., 1995) in the pulse width modulation (PWM) technique a low frequency reference waveform ($v_{control}$) is compared against a trigonal waveform with frequency (switching frequency f_s) equal to the desired operating frequency as it is demonstrated in figure 2.9

The switching frequency f_s dictates the frequency with which the inverter's switches change state. Both f_s and V_{tri} have stable width. The resulting voltage waveform in the inverter's output will be a sinusoidal waveform with harmonic distortion in the switching frequency sidebands and its multiples, as shown in figure 2.10.
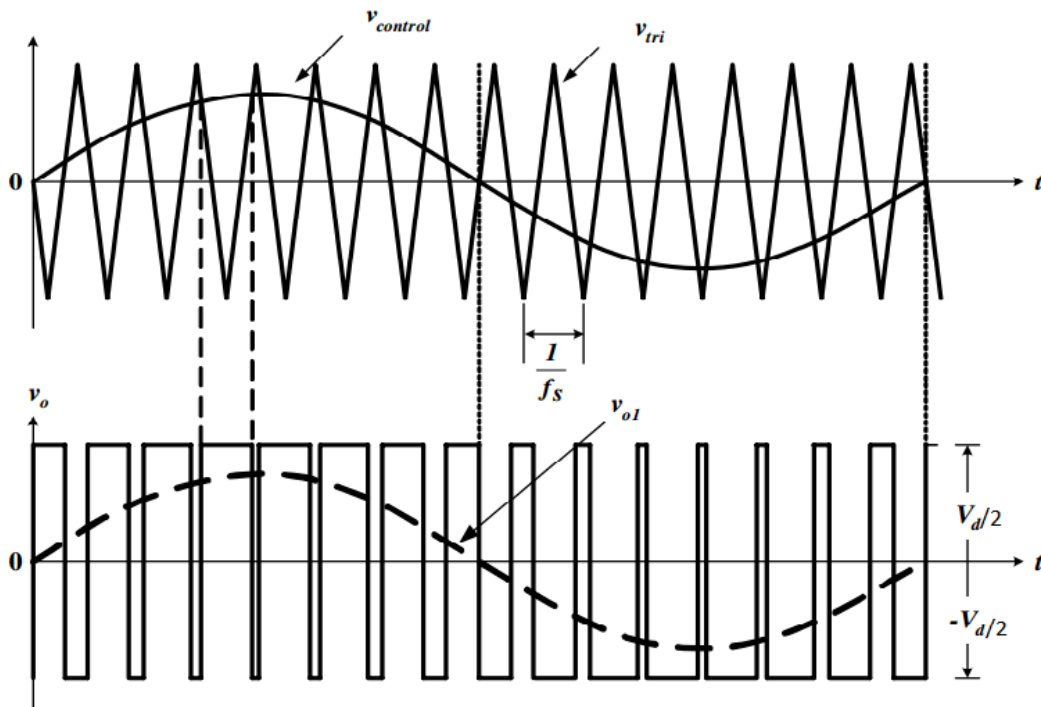
Figure 2.9 SPWM. Source: (Mohan, et al., 1995)

Two crucial elements of the pulse width modulation technique are:

1. the amplitude modulation ratio (m_a) equal to $\dfrac{V_{control}}{V_{tri}}$.

For a single phase inverter the output voltage is equal to $\dfrac{V_{control}}{V_{tri}} \sin \omega t \dfrac{V_d}{2} = m_a \sin \omega t \dfrac{V_d}{2}$ considering the waveform's amplitude equal to $m_a \dfrac{V_d}{2}$ it can be concluded that on condition that $m_a \leq 1$ the inverter's output voltage has a linear relationship with m_a.

2. the frequency modulation ratio (m_f), equal to $\dfrac{f_s}{f_1}$.

The frequency modication factor is preferable an odd number in order to create an odd symmetry (f(t)=-f(t+Ts/2)) and eliminate the even harmonic bands[1].
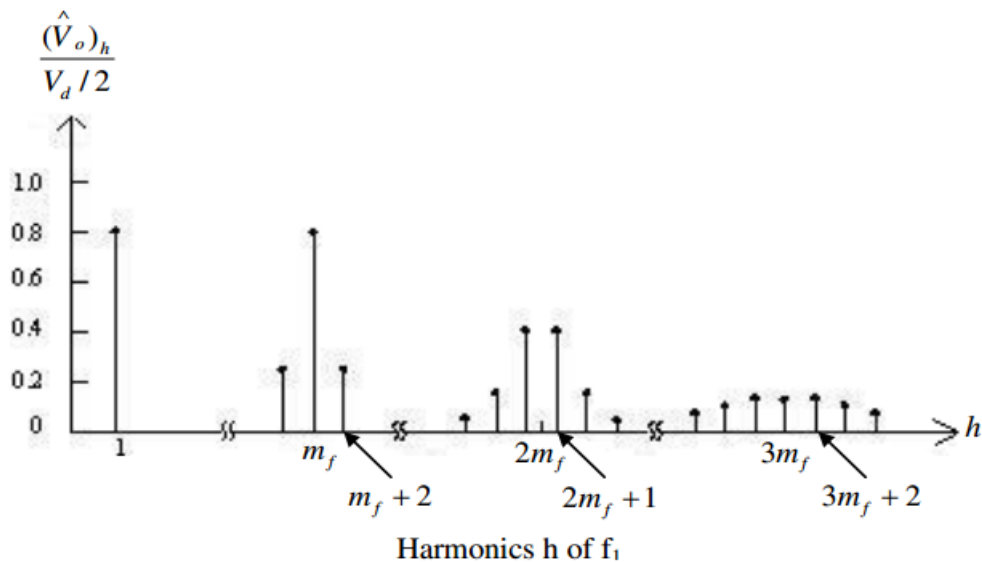
Figure 2.10 Source: (Mohan, et al., 1995)

A technique that can be used along with PWM is the third harmonic injection, according to which a third harmonic component is added to the modulating waveform in order to increase the fundamental voltage. This method is used to overcome over-modulation ($m_a>1$) which causes a reduction in the number of pulses in the line-to-line voltage waveform leading to the generation of low order harmonics (e.g. 5th, 7th) *(Yazdani & Iravani, 2010)*.

---

[1] Only harmonics in multiples of 3 will remain for a three phase inverter.

2.5 Harmonics: causes and mitigation methods

Voltage and current harmonics are distorted parts of the sinusoidal voltage and current waveforms that can be analysed in multiples of the system's fundamental frequency and usually occur when a sinusoidal voltage source is connected to a non-linear load or system component (Arrillaga & Watson, 2003).

Figure 2.11 as presented in (Arrillaga & Watson, 2003) demonstrates the difference between the power flow in fundamental and harmonic frequency.

In the former case (figure 2.11 (a)) most of the power is transmitted to the load R_l and only a small fraction of it is dissipated in the converter (P_{c1}) and the system's impedance (P_{s1}). In the latter case (figure 2.11 (b)) the generator's electromagnetic field (e.m.f.) is short circuited hence the generator and the transmission line are relpaced by their harmonic impedances; the converter acts as a harmonic current source (I_h) and a fraction of this current is dissipated in the load and the line's and generator's harmonic impedances (P_{1h}, P_{gh}, P_{sh}). Thus the overall losses consist of the
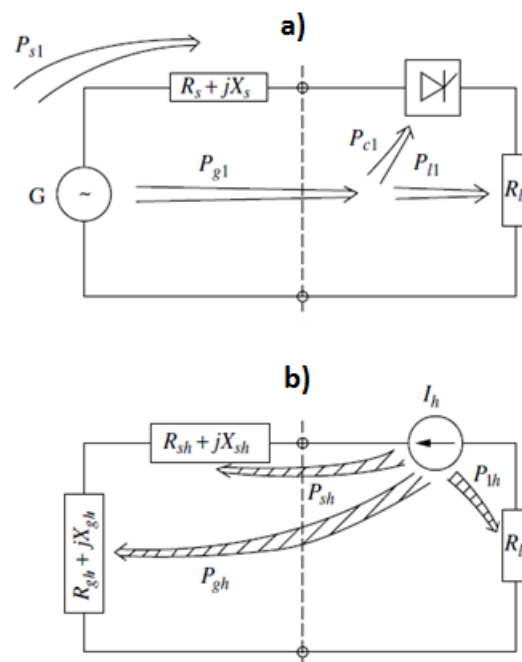
Figure 2.11 Comparison of power flow at fundamental and harmonic frequency (Arrillaga & watson, 2003)

losses in fundamental frequency and in harmonic frequency.

The harmonic content in a power system is assessed using the percentage of Total Harmonic Distortion (%THD) in voltage and current waveforms. According to (Mohan, et al., 1995) this is calculated by the fraction of the rms distorted value e.g. I_{dis} over the waveform of the fundamental frequency, I_{s1}. More specifically:

$$I_s = (I_{s1}^2 + \sum_{h \neq 1} I_{sh}^2)^{1/2}$$

$$I_{dis} = [I_s^2 - I_{s1}^2]^{1/2} = (\sum_{h \neq 1} I_{sh}^2)^{1/2}$$

$$\%THD = 100 \cdot \frac{I_{dis}}{I_{s1}}$$

Harmonics are typically generated by non-linear loads; namely, any kind of variable frequency/speed drives, UPS unit, fluorescent lighting ballasts etc. can cause such phenomena.

Several areas can be affected by current and voltage harmonics. First of all, harmonic currents can cause over-heating and fatigue of the neutral conductor, as those which are odd multiples of the fundamental add in instead of cancelling out each other. Serious effects are also observed at transformers since they lead to increased eddy losses which result in high operating temperature and consequently severe reduction of their lifetime. Additionally, tripping nuisance can occur to circuit breakers and skin effect is significant in high frequencies. Harmonic voltages can affect induction generators resulting in increase of losses (same as transformers) and also cause electromagnetic interference on zero-crossing controllers.

The main harmonic mitigation methods are the application of filters (active and passive) and the use of isolation transformers. The rationale behind passive filters is to provide a low impedance path to harmonic currents so that they will flow in the filter and not in the electrical network. Passive filters can be tuned in a specific frequency or for a broadband depending on the requirements. Isolation transformers are zig-zag transformers, which are used to block triple-N harmonics in their windings and isolate them from the supply. Active filters are used as a more sophisticated solution when

the harmonic content is less predictable. Among those methods, the one of passive filters is the most commonly used as it is cheaper and simpler.

2.6   Harmonic filters

A passive filter consists of a combination of resistors, capacitors and inductors and it aims to differentiate between wanted and unwanted frequencies by providing low impedance paths in order to alter signal waveforms (Thede, 2004). Passive filters are most commonly classified by their frequency selectivity. In terms of selectivity the filters are characterised by their gain and attenuation, as well as their pass-band and stop-band.

The pass-band is simply the range of frequencies that can pass through the filter with minimal change in amplitude; the edge of the pass-band is called cut-off frequency and it's also known as 'half power point' because a 3dB amplitude reduction occurs (Winder, 2002). The respective range of reduced frequencies that will effectively be cut-off is the stop-band.

The four main types of filters in terms of frequency selectivity are the following:

- Low-pass filter (LPF), which allows the low frequencies to pass through and eliminated the high frequencies.

- High-pass filter (HPF), which has a stop-band until a specific frequency and then a pass-band from this frequency to infinity.

- Band-pass filter (BPF), which passes only a band of frequencies and attenuates the rest.

- Band-stop filter (BSF), which attenuates a band of frequencies located between two pass-bands.

Figure 2.12 demonstrates the filter response and specifications for the above mentioned kinds of filters.
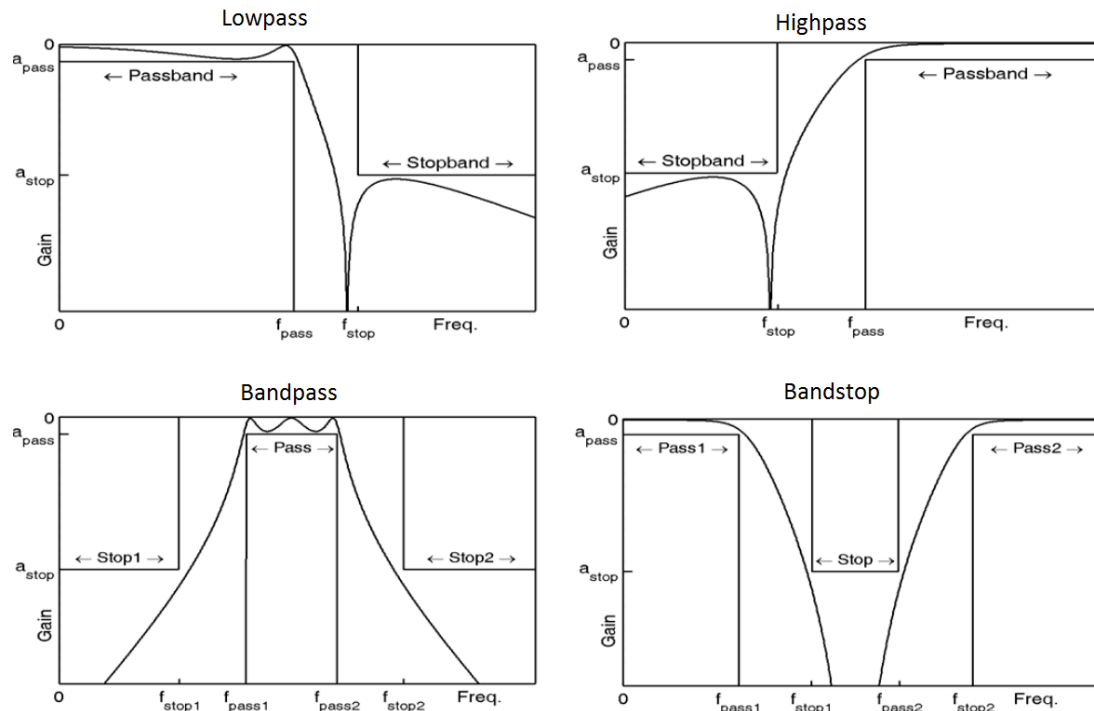
Figure 2.12 Filter specifications. Source: (Thede, 2004)

The ratio of output to input signal amplitude represents the signal's gain, if it's over 1, or attenuation if it's bellow 1. As stated in (Thede, 2004) the gain/attenuation response of a filter is has a wide range so it is typically expressed in a logarithmic scale to enhance accuracy for small values in the stop-bands:

$$gain_{dB} = 20\log(gain)$$
$$attn_{dB} = 20\log(gain^{-1}) = -gain_{dB}$$

According to (Rosa, 2006) for single tuned filters, the filter's resonant frequency is given by the formula $f_0 = \dfrac{1}{2\pi\sqrt{LC}}$, where f_0 is the resonant frequency and L and C are the filter's inductance and capacitance respectively.

As passive filters provide reactive compensation in addition to eliminating undesired frequencies they are usually designed suitably for both filtering and improving the power factor.

The hierarchy of the steps that need to be followed for the design of a harmonic filter for the grid side of a power system can be summarised as:

1. Calculate the capacitance required in order to enhance the power factor

2. Estimate the reactor required to tune the series capacitor at the harmonic frequency

3. Calculate the peak capacitor voltage and reactor current

The impedance of a harmonic filter branch is calculated as $Z = R + j[\omega L - \frac{1}{\omega C}]$ where ω is the angular frequency of the power system.

2.7 Subsea cables

Subsea cables linking the offshore tidal generator to the utility grid onshore can cause harmonic parallel resonance because of the cable's considerable shunt capacitance, especially when some resonance bands are interacting with the harmonics injected by the system's frequency converter (Liang & Jackson, 2008).

A common manner to mitigate resonance and attenuate harmonics is the application of single tuned harmonic filters in the 5th 7th 11th and 13th order harmonics according to (McLean, et al., 1993).

3 Model description

A model that would represent the whole system can be seen in figure 3.1(b) and it can be compared to the single line diagram of the system, as presented before, in figure 3.1(a); here the grid side of the tidal system is also taken into consideration. However, this study focuses on the machine side of the system, hence the model that was used

for the conducted analysis can be seen in figure 3.2 ; it consists of the generator, the subsea cable, the transformer and the machine side of the frequency converter along with a 3-phase output reactor. The simulations are run for 7 seconds in order for the system to reach steady state and the type of simulation used is discrete simulation with a fixed time step of 2.5μsec. A detailed description of the system components is given bellow.
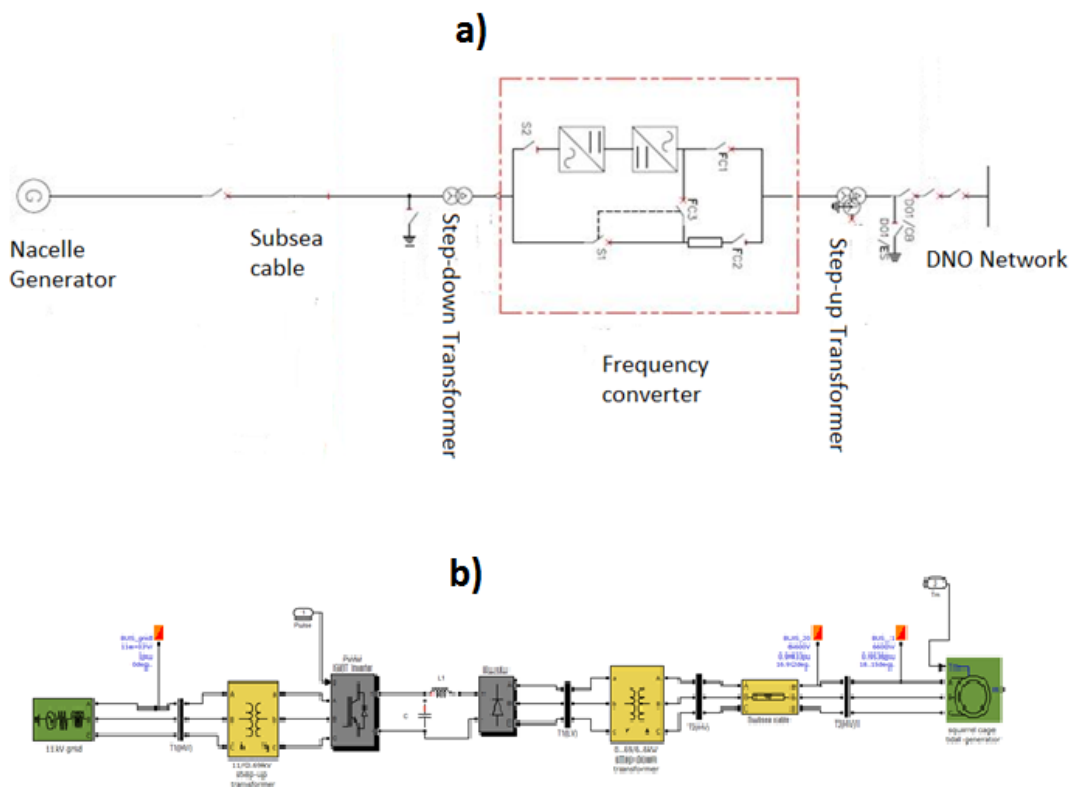
Figure 3.1 (a) Single line diagram (b) System representation in Simulink including the grid side
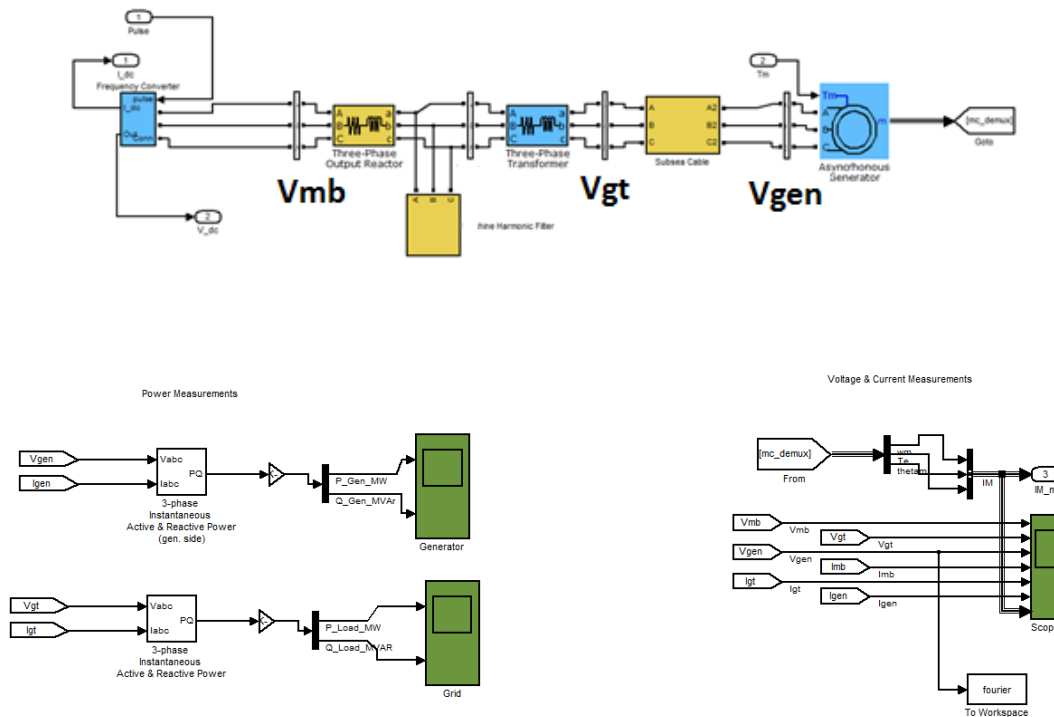
Figure 3.2 Simulated system and measuring blocks

The model's operation is simplified; one flow speed scenario is examined (2.6m/sec), which leads to a torque output and a constant modulation index in the converter. Additionally, the transformer is modelled as a series resistive-inductive branch and all the result values are referred to the LV.

Voltage and current measurements are taken in the four busbars, i.e.:

- V_{gen} & I_{gen}, displaying the peak-to-peak generator output

- V_{gt} & I_{gt} displaying the voltage and current after the subsea cable

- V_{abc} & I_{mb} displaying the voltage and current just before the output reactor

- $V_{mb,}$ the voltage before the converter

The real and apparent power that is generated/ absorbed is measured in the generator output and after the subsea cable.

3.1   Component details

3.1.1   Induction Generator

A squirrel cage 3 pole pair induction generator is modelled, with rated power of 1455kVA and rated output voltage of 6.6kV. The voltage and current output of the generator can be viewed in figure 3.3 and its real and reactive power output are displayed in figure 3.4
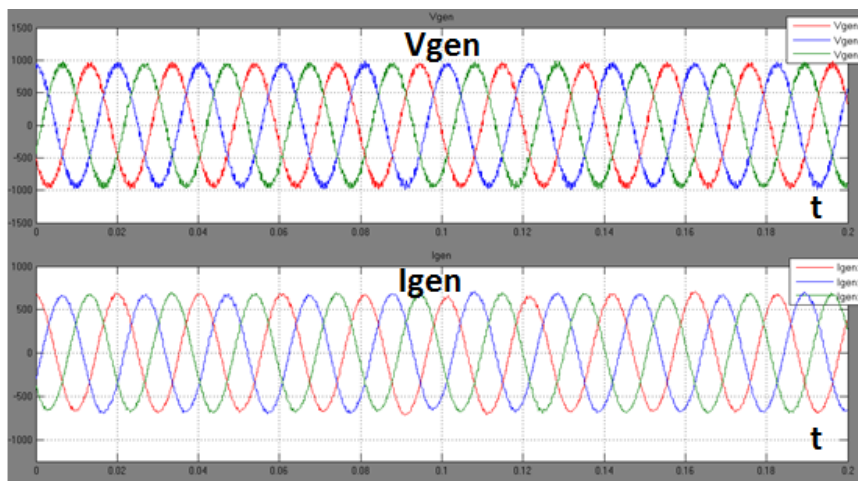
Figure 3.3 Generator's output voltage and current
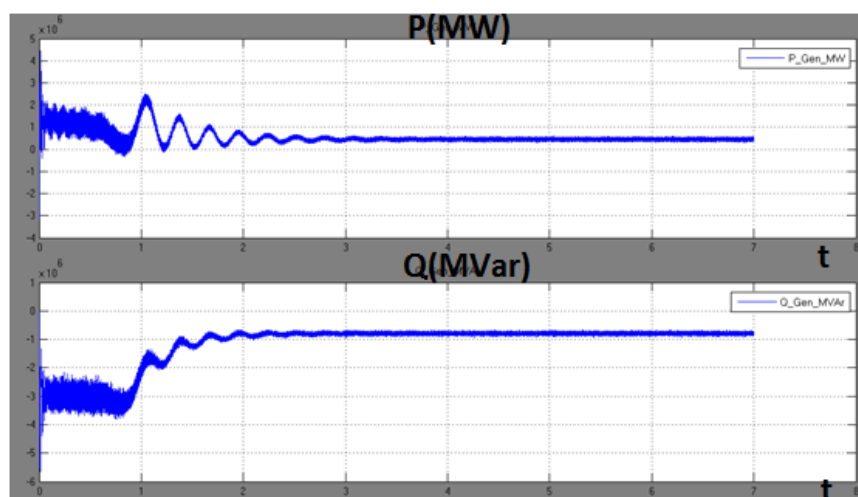
Figure 3.4 Generator's output real and reactive power

As it can be observed in figure 3.4 the generator's the initial subtransient state is barely visible as it lasts for some tens of milliseconds, then transient state lasts about 2.5 seconds and then the system eventually reaches steady state.

3.1.2 Subsea cable

The subsea cable was modelled as a 3 phase Π section line. The number of Π sections used (N) was calculated by the formula displayed bellow, as advised in Simulink's guidelines:

$$N = \frac{f_{max} \cdot 8 \cdot l_{total}}{v}$$

Where f_{max} is the maximum frequency range that can be assessed, l_{total} is the total length of the cable and v is the propagation speed which is equal to $\frac{1}{\sqrt{LC}}$ and is referred to the cable characteristics (inductance and capacitance per km.)

In the examined system the maximum frequency that is assessed is 6 kHz, which is a bit above double the converter's switching frequency.
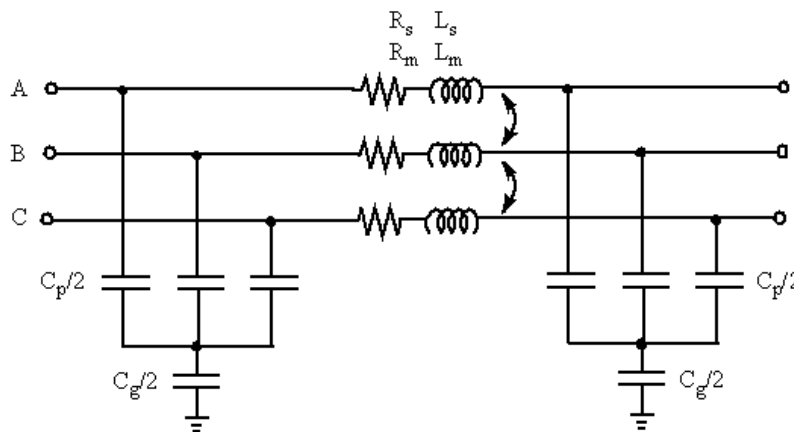
Figure 3.5 Circuit representation of a three-phase PI section line

3.1.3 Transformer

The system includes a Δ-Y transformer which steps the generator's voltage from 6.6kV down to 690V which is the converter's rated voltage. The transformer's nominal parameters along with the calculations of its series and magnetising resistance and inductance are available below:

Nominal Power	1200 kVA	Vector	Dy11
Frequency	50 kVA	Z%	10
$V_{nom(HV)}$	6.6 kV	Load loss	13 kW
$V_{nom(LV)}$	0.69kV	No load loss	2 kW

Analysis:

$$a = \frac{6600}{690/\sqrt{3}} = 16.567 \Rightarrow a^2 = 274.48$$

Primary line current I_{1L}:

$$I_{1L} = \frac{1200 \cdot 10^3}{\sqrt{3} \cdot 6.6 \cdot 10^3} = 104.97A$$

Primary phase current I_{1ph}:

$$I_{1ph} = \frac{I_{1L}}{\sqrt{3}} = \frac{62.98}{\sqrt{3}} = 60.60A$$

Secondary current:

$$I_{2L} = I_{2ph} = \frac{1200 \cdot 10^3}{\sqrt{3} \cdot 690} = 1004A$$

From open circuit test:

$$P_{Fe} = \frac{V^2}{r_{Fe}} \Rightarrow r_{Fe} = \frac{(690/\sqrt{3})^2}{2000} = 79.35\Omega$$

$$R_{Fe} = a^2 \cdot r_{Fe} = 21.78k\Omega$$

$$I_{Fe} = \frac{690/\sqrt{3}}{79.35} = 5.02A$$

$$I_M = \sqrt{I_2^2 - I_{Fe}^2} = \sqrt{1004^2 - 5.02^2} = 1003.98A$$

$$X_{2M} = \frac{690/\sqrt{3}}{1003.98} = 0.397 \Rightarrow L_{2M} = \frac{0.397}{100\pi} = 0.00126H$$

$$L_{1M} = a^2 \cdot L_{2M} = 0.346H$$

From Short circuit test:

V_b=6.6kV S_b=1200kVA I_b=I_{ph}=60.60A Z_b= V_b/I_b=6600/60.60=108.91Ω

$$Z = Z_b \cdot 0.1 = 10.891\Omega$$

$$R_{s1} = \frac{P_{Cu}}{I_1^2} = \frac{13000}{60.60^2} = 3.54\Omega$$

$$X_{s1} = \sqrt{Z^2 - R_{s1}^2} = 10.3\Omega \Rightarrow L_{s1} = 0.0328H$$

$$R_{s2} = \frac{R_{s1}}{a^2} = 0.0129\Omega$$

$$L_{s2} = \frac{L_{s1}}{a^2} = 1.194 \cdot 10^{-4}H$$

The 6.6/0.69 kV transformer is modelled as an inductive resistive branch for simplification so that the numerous simulations will require less time to run. Hence the transformer's series resistance and inductance referred to the LV are used in the model.

3.1.4 Machine filter

The machine filter that was applied and tested consists of an LC and an RC branch. The resonant frequency is tuned by varying the LC branch's values:

$$2 \cdot \pi \cdot f_{res} = \frac{1}{\sqrt{LC}} \Rightarrow \sqrt{LC} = \frac{1}{2 \cdot \pi \cdot f_{res}} \Rightarrow LC = \left(2 \cdot \pi \cdot f_{res}\right)^{-2}$$

The values of capacitance and inductance of the LC product were defined through trial and error procedure for each resonant frequency.
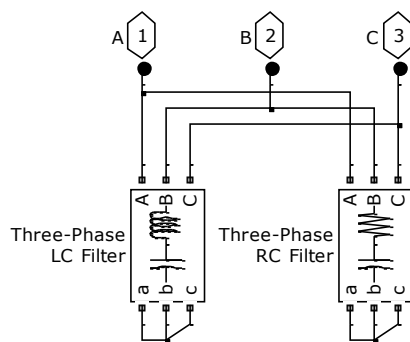
Figure 3.6 Harmonic filter

3.1.5 Output Reactor

The output reactor is used in combination with the harmonic filter for the mitigation of detrimental effects due to high harmonic content (VanderMeulen & Maurin, 2010). It consists of a resistive-inductive branch.

3.1.6 Other components

3.1.6.1 Bus bars

There are four bus bars in the model, in order to get voltage and current phase-to-phase measurements in points of interest, as explained in figure 3.2.

Finally, the voltage and current waveforms in design operating condition are illustrated bellow; magnified pictures of the waveforms for better observation are provided at the end of Appendix B (p.55-56). It can be observed from figure 3.7 that voltage and current waveforms show minimal ripple, with current waveforms being less distorted than the voltage waveforms, as expected. Figure 3.8 illustrates, again, the difference between transient and steady state.
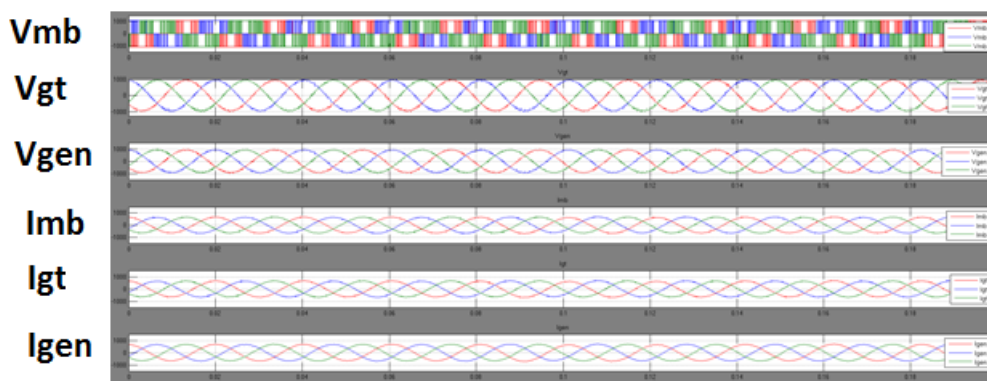
Figure 3.7 Voltage and current waveforms
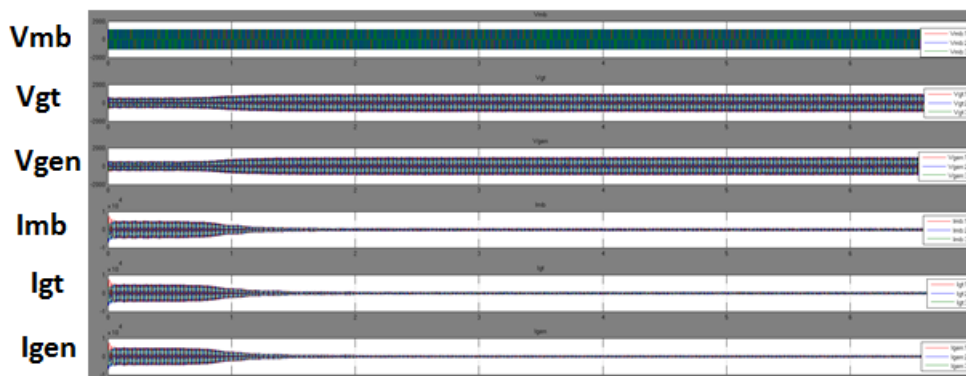
Figure 3.8 Scaled waveforms

4 Simulations and results

The simulation results were assessed judging from the percentage of voltage total harmonic distortion (%THD) in the three phases at the generator output ($V_{gen)}$) and at the transformer output (V_{gt}). The percentage of current total harmonic distortion was in all cases lower than the one referring to voltage. The phase shown every time from now on will be the one that represents the worst case scenario, i.e. the phase that shows the highest %THD. The sampling time is equal to 10 cycles starting from t=6.7 seconds, when the system has already reached steady state, as indicated in figure 4.1.
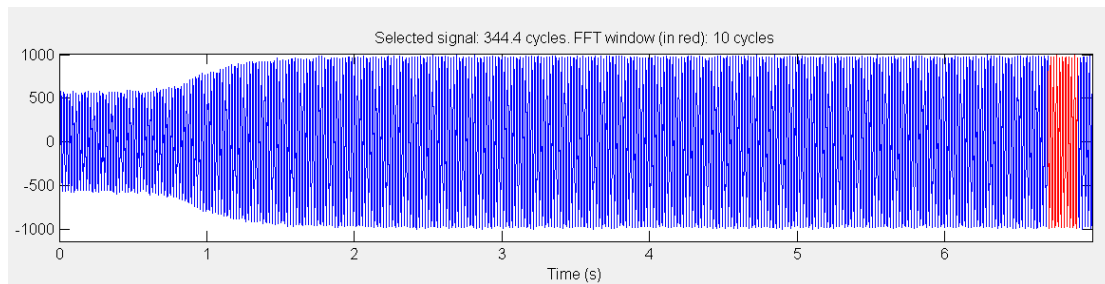
Figure 4.1 Selected signal

Figures 4.2 to 4.4 demonstrate the results from running simulations with 'normal operating conditions' (initial design characteristics for the transformer and output reactor and rated frequency for the respective flow speed) and an applied filter tuned near the switching frequency (2550 Hz).
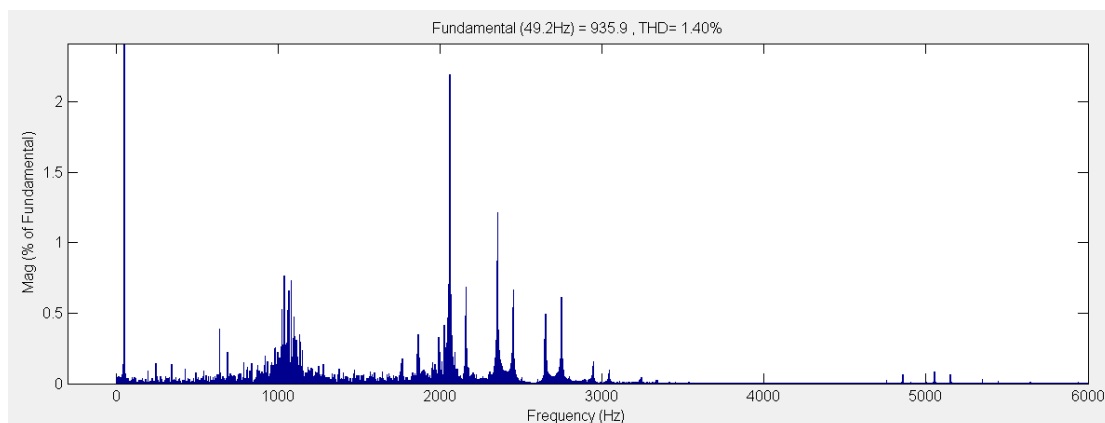
Figure 4.2 FFT analysis for V_{gt}
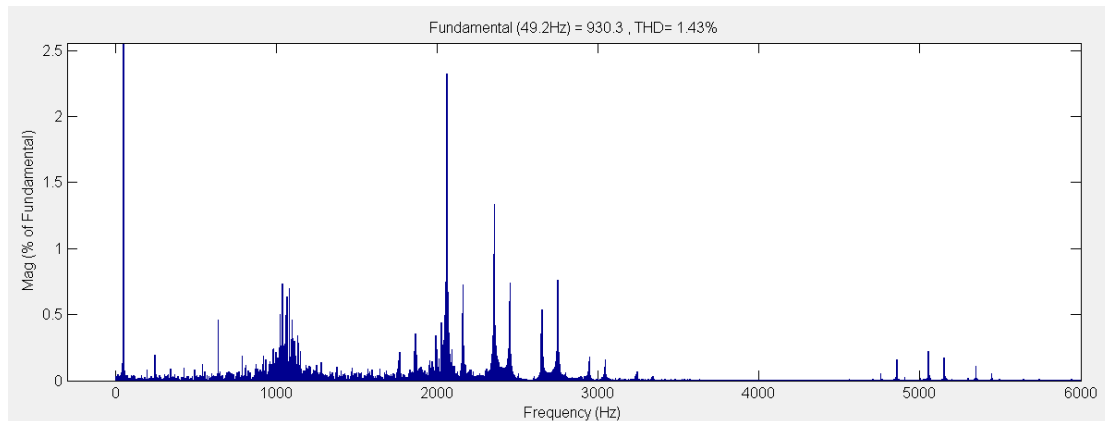
Figure 4.3 FFT analysis for V$_{gen}$

It can be observed from figures 4.2 and 4.3 that harmonics with significant magnitude are found near the switching frequency and its multiples. The difference between V$_{gt}$ and V$_{gen}$ is minimal; namely, the former shows slightly more intense harmonic distortion near 1kHz whereas the latter is more distorted around the double of the switching frequency. In figure 4.4 the harmonic distortion is seen as ripple in the voltage waveform. Again, the difference between the two outputs is insignificant.
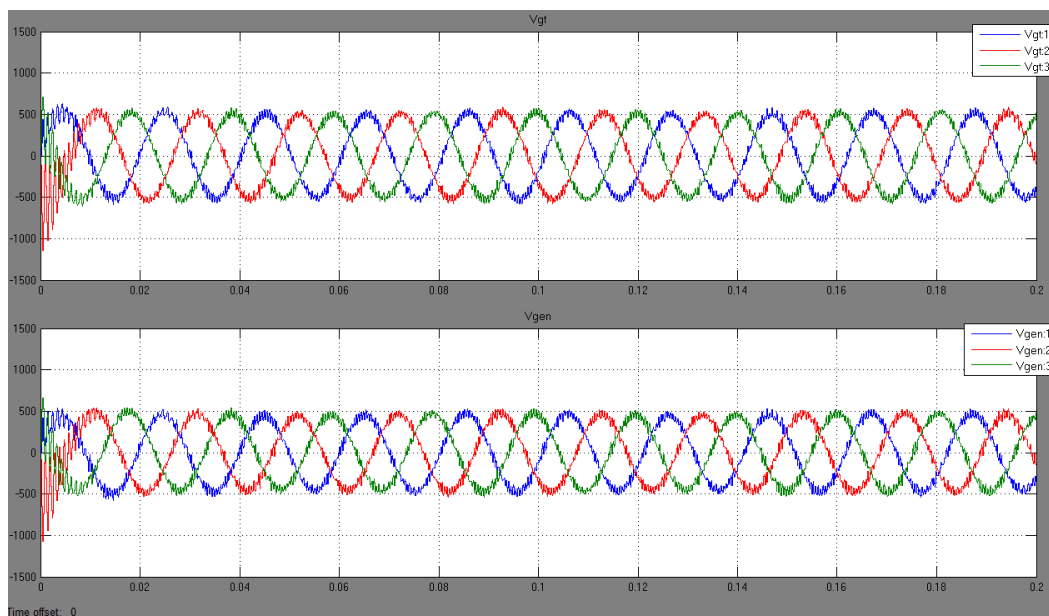
Figure 4.4 Voltage waveforms

4.1   Varying inductance

In an attempt to identify what factors affect the harmonic distortion and in what way as well as whether there is any resonance between components of the system or not, the output reactor's and the transformer's inductance where changed.

Changing the output reactor's inductance from 40μH to 110 μH (with 90μH being the initial value) suggested that the inductance and %THD are inversely proportional, as illustrated in figure ; while the 3% permitted threshold was only exceeded for the case of 40μH.
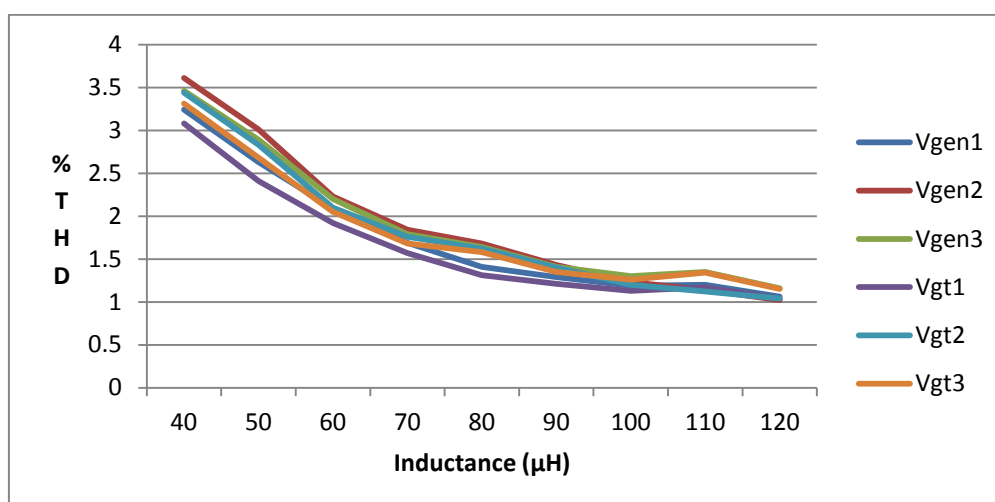
Figure 4.5 Output reactor's inductance Vs %THD

Increasing the transformer's inductance from 3μH to 6mH (with the original value being 100 μH) indicated that a radical increase in %THD occurs for the values between 30μH and 60μH. Namely, the peak value for 50μH was 32.72% as shown in figure 4.6. This phenomenon suggests that there is resonance between two or more system components. Altering the output reactor's inductance and maintaining the transformer's inductance at 30μH, then at 40μH and then at 50μH it was observed that although the %THD was affected a resonance between those two impedances couldn't have been the cause of these peak values as for no value is the harmonic content in permitted levels. Indicatively, figure 4.7 shows how %THD is affected when the transformer's inductance is kept at 50μH and the output reactor's inductance is varied.
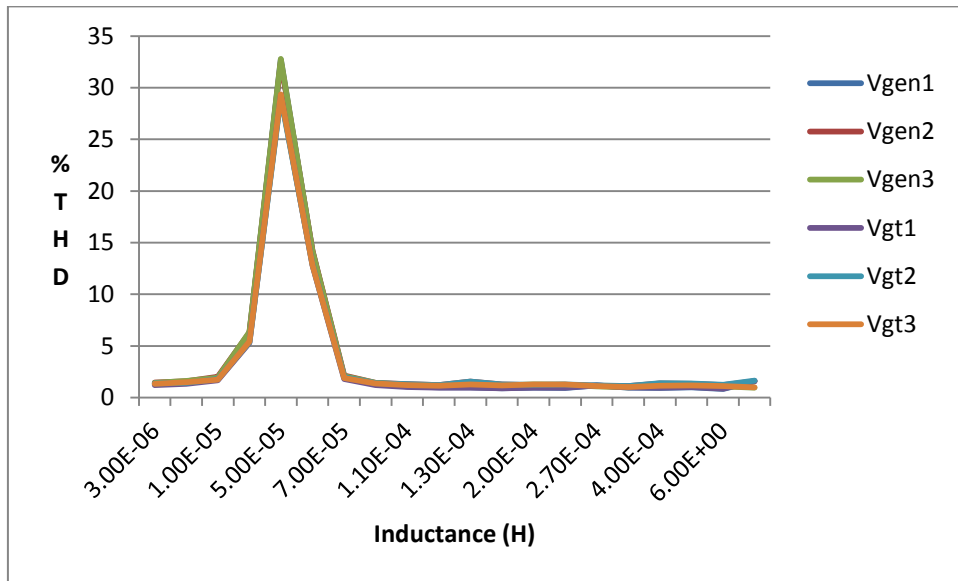
Figure 4.6 Transformer's inductance Vs %THD
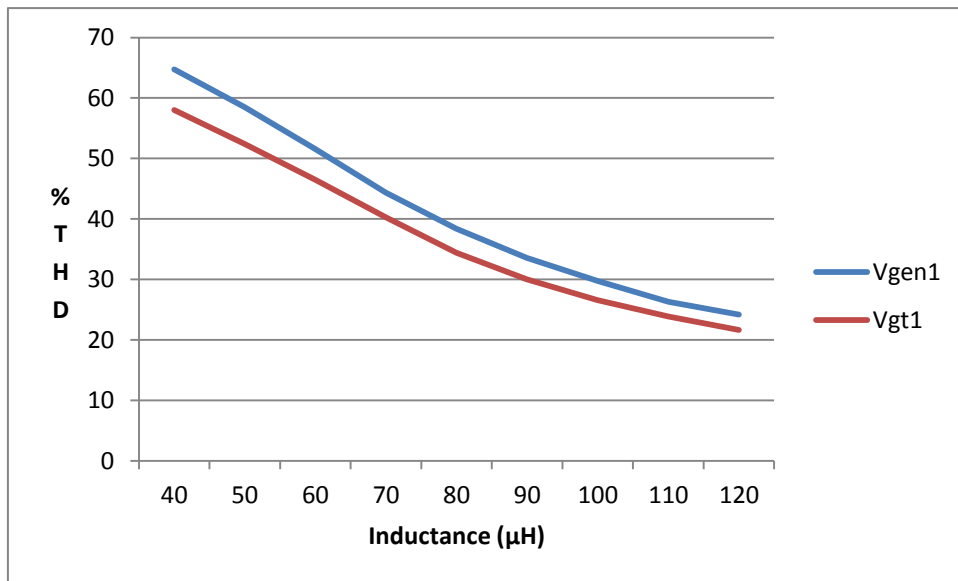
Figure 4.7 %THD for V_{gen1} and V_{gt1} with varying inductance in the output reactor

4.2 Varying the cable length

The subsea cable's length was varied in order to investigate the difference in harmonic content in a tidal array system, where tidal generators would have different distance from shore.

Table 4-1 illustrates that the percentage of total harmonic distortion is slightly affected by the change in cable length and that cable length and %THD are inversely proportional. Another observation from these results, more related to the software, was that the change in %THD was rather affected by the change in PI sections number, than the change of actual cable length.

Table 4-1 %THD with varying length

		%THD					
PI sections	overall length	Vgen1	Vgen2	vgen3	Vgt1	Vgt2	Vgt3
2	3	2.05	2.24	2.20	1.91	2.10	2.06
3	3.5	1.27	1.27	1.49	1.23	1.22	1.47
3	4	1.27	1.27	1.49	1.23	1.22	1.47
3	4.5	1.27	1.27	1.49	1.23	1.22	1.47
3	5	1.27	1.27	1.49	1.23	1.22	1.47
4	5.5	1.52	1.40	1.26	1.51	1.38	1.22
4	6	1.52	1.40	1.26	1.51	1.38	1.22
4	6.5	1.52	1.40	1.26	1.51	1.38	1.22
4	7	1.52	1.40	1.26	1.51	1.38	1.22
5	7.5	1.25	1.47	1.46	1.24	1.48	1.46
5	8	1.25	1.47	1.46	1.24	1.48	1.46
5	8.5	1.25	1.47	1.46	1.24	1.48	1.46
5	9	1.25	1.47	1.46	1.24	1.48	1.46
6	9.5	1.35	1.91	1.57	1.35	1.95	1.59
6	10	1.35	1.91	1.57	1.35	1.95	1.59

4.3   Changes in filter

The harmonic filter was modified to be optimised in one hand, and in order to investigate which harmonic orders cause significant distortion on the other hand. Simulations indicated that tuning the filter away from the switching frequency elevated the percentage of total harmonic distortion. Figure 4.8 illustrates how the percentage of total harmonic distortion changes when tuning the filter to low order frequencies and then higher order frequencies. It is observed that there is approximately 1% difference between the %THD measured in the generator output and the one measured after the step-down transformer. The percentage of THD decreases when the filter is tuned to the 7th and 11th harmonic order and then steadily increases.
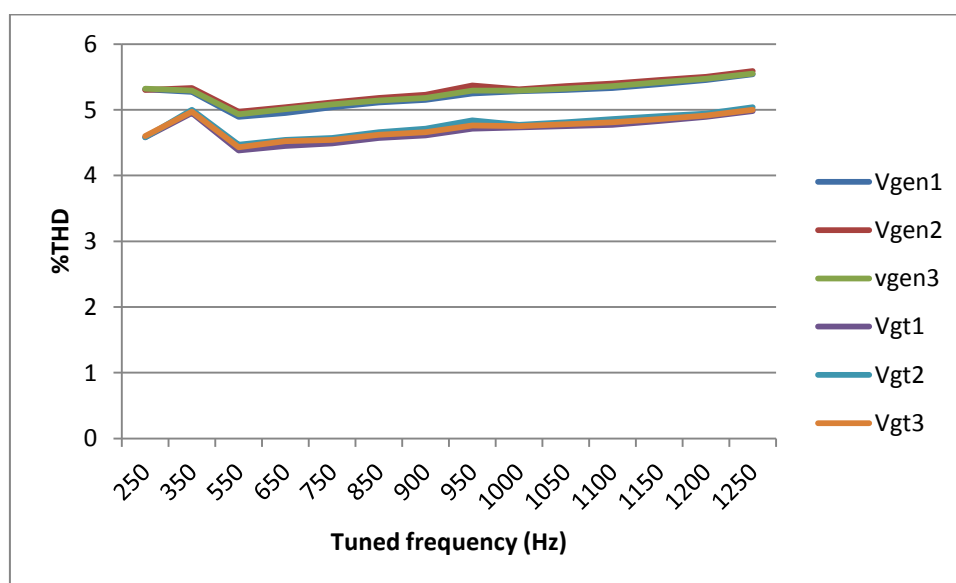
Figure 4.8 Relation between %THD and filter's tuning frequency

Figure 4.9 demonstrates how the percentage THD is affected as the filter is tuned closer to the switching frequency. The %THD decreases to permitted levels and reaches minimum (1.67%) when the filter is tuned to the switching frequency. After this point, as the tuned frequency increases, the %THD rises as well. Additionally, it can be observed that although until the 46th harmonic (2300Hz) the difference in

%THD between V_{gen} and V_{gt} voltages is kept at approximately 0.5%, after this point there is no distinctive difference between the two of them.
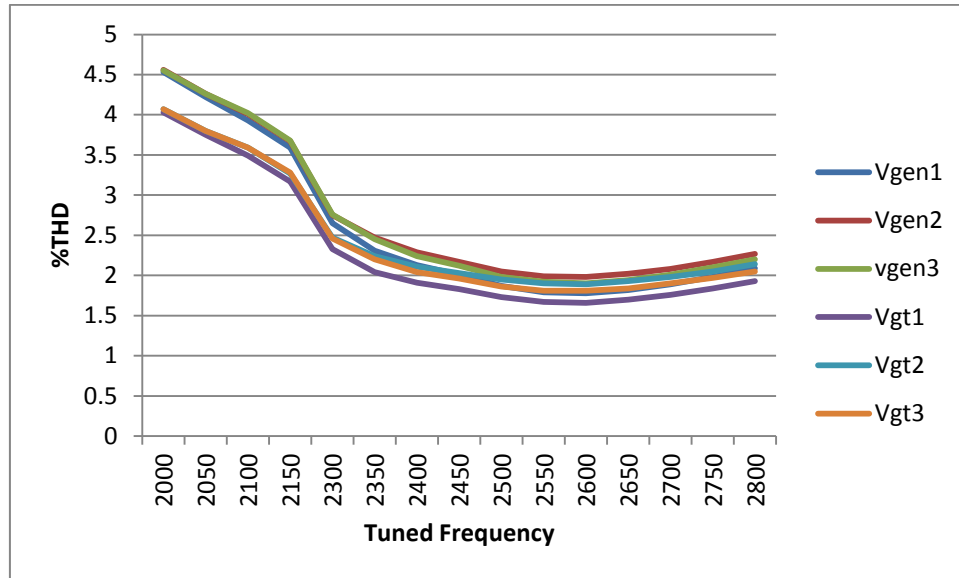
Figure 4.9 Relation between %THD and filter's tuning frequency

In figures 4.10 to 4.13 the harmonic content in cases of different applied filters can be compared and assessed. What can be seen from this harmonic analysis is that the orders that cause harmonic distortion are the same in both cases, but are better mitigated when the filter is tuned at the 51st harmonic, meaning that harmonic orders near the switching frequency cause more distortion than the low order harmonics. The differences between the harmonic content of V_{gen} and V_{gt} is, in all cases, insignificant.
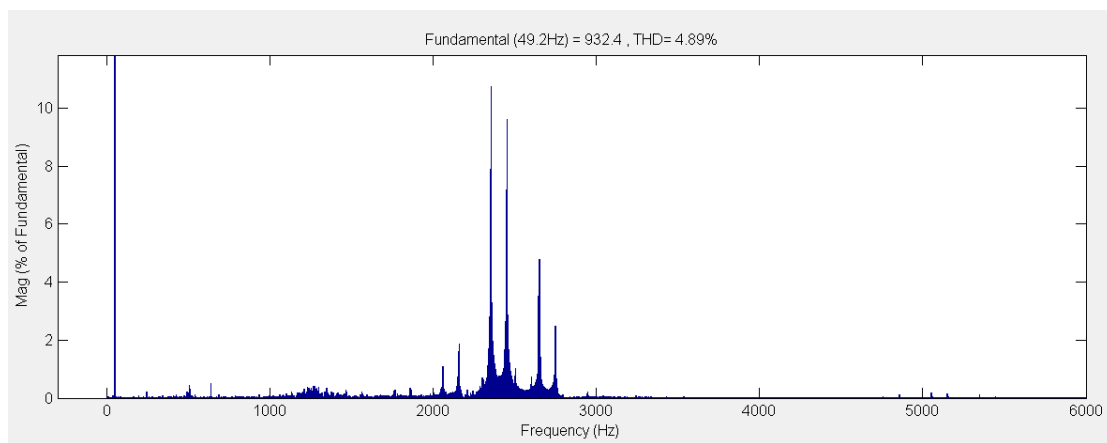
Figure 4.10 Harmonic content in Vgen1. Filter tuned at 11th harmonic

Fundamental (49.2Hz) = 937.4 , THD= 4.38%
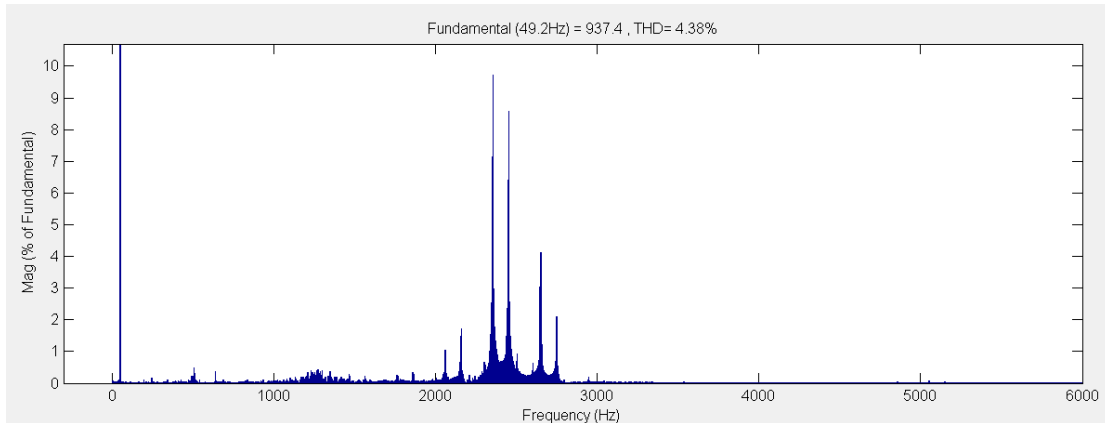
Figure 4.11 Harmonic content in Vgt1. Filter tuned at 11th harmonic

Fundamental (49.2Hz) = 930.2 , THD= 1.79%
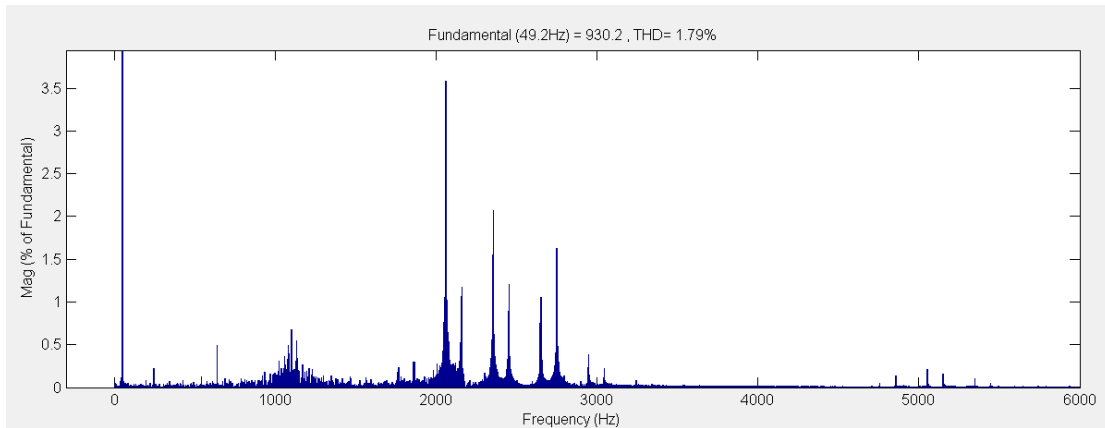
Figure 4.12 Harmonic content of Vgen1. Filter tuned at 51st harmonic

Fundamental (49.2Hz) = 935.8 , THD= 1.67%
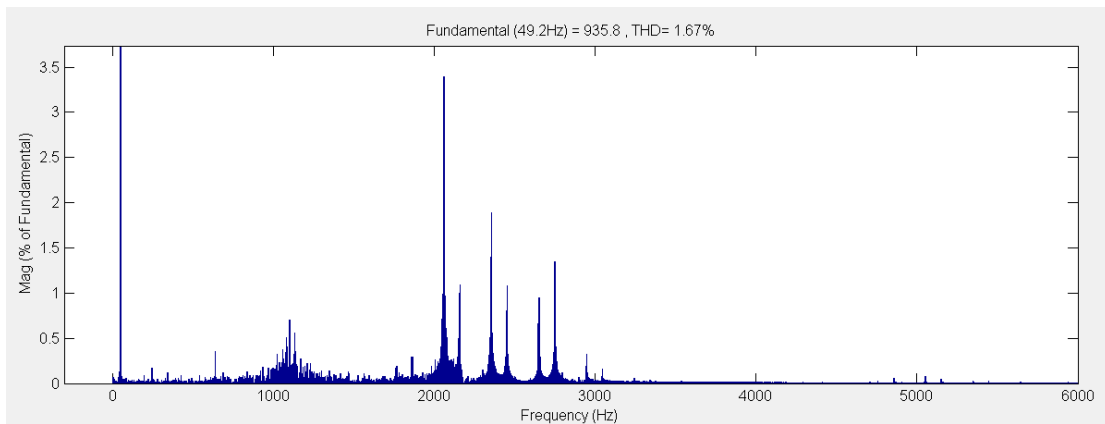
Figure 4.13 Harmonic content of Vgt1. Frequency tuned at 51st order

Figures 4.14 and 4.15 demonstrate how differently the voltage waveforms appear due to the voltage harmonic distortion.
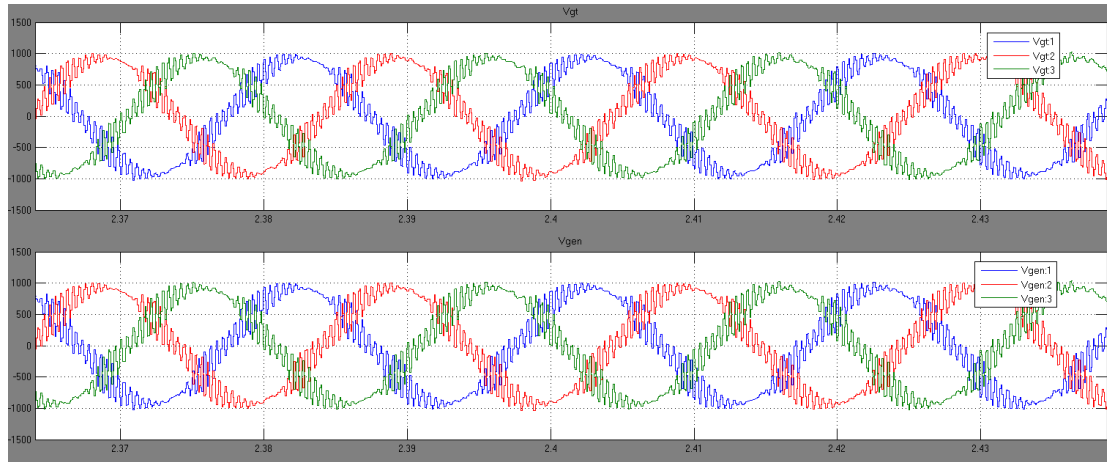
Figure 4.14 Voltage waveforms for filter tuned at the 11th harmonic
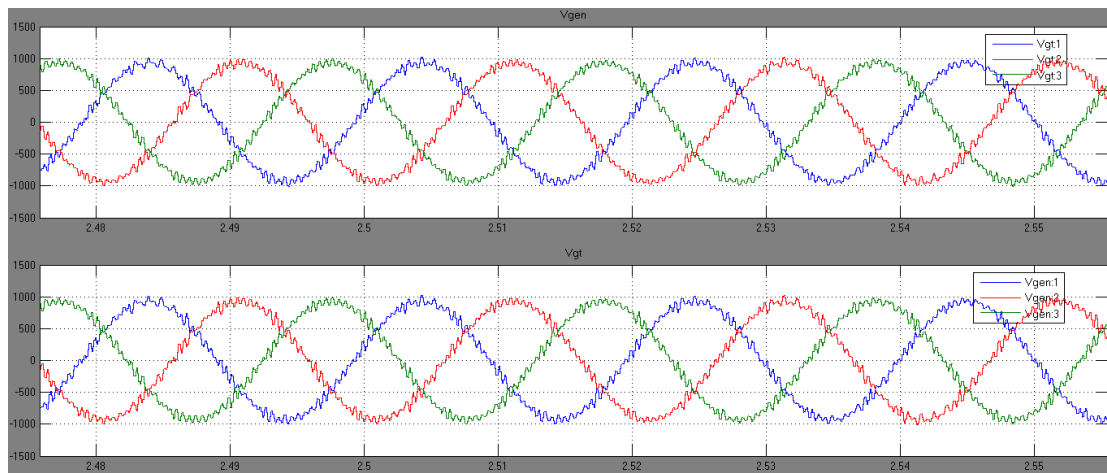
Figure 4.15Voltage waveforms for filter tuned at the 51st harmonic

The conclusions that were reached after these simulations can be summarised as follows:

- The transformer's magnetising inductance as well as the output reactor's inductance are inversely proportional to the %THD.

- The cable is varied to an extend that causes insignificant effect to the harmonic content at the machine side of the system.

- Elevated percentage of THD is observed when the harmonic filter is tuned away from the frequency converter's switching frequency; thus, the frequency converter is the main source of harmonics in the system.

4.4 Proposed methodology

A design algorithm is proposed for the application of machine side filters in a tidal facility. After the system's specifications are defined; i.e. the installed capacity, type of generator, distance from shore, converter's operating voltage to know whether it requires a transformer or not etc. A model suitable to represent the desired system should be built and run first in order to view the harmonic content in the considered normal operating conditions. After this stage, the sensitivity analysis is performed by changing the model's parameters such as the transformer's impedance characteristics, the cable's impedance characteristics and length, or the converter's switching frequency. This stage should give a clearer picture of the system's resonances and effects on harmonics and harmonics spectra that need to

Build model

Apply changes separately

Apply combined changes

View harmonic content of all considered possibilities

Design filter

Apply filter & view new harmonic content

Optimise filter according to results
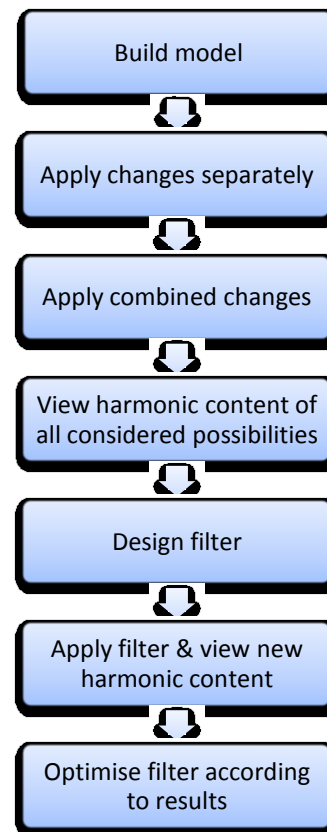
Figure 4.16 Filter design algorithm

be mitigated can be initially defined. Then, system changes can be applied simultaneously in different combinations, dictated by the previous results so that additional information about the system can be obtained. Now that information about harmonic sidebands is more solid a passive filter can be designed; the type of the filter (i.e. single/double tuned, low pass, band pass etc.) will be determined by which harmonic orders need to be eliminated. After the filter is designed the same simulations should be run again in order to compare results after the filter's application. Finally, after its first application, the filter can be altered in order to be optimised by changing its characteristics and comparing simulations.

5 Conclusions and recommendations for further research

Judging from the results of the simulations during the conduction of this thesis it can be concluded that in the machine side of a tidal system harmonics with significant magnitude occur at the converter's switching frequency, as well as close to its multiples and its sidebands. Thus, a satisfactory mitigation method would be to apply a passive filter tuned to the switching frequency. In order to avoid system resonances that can cause further harmonic distortion as well as over-voltages and over-currents a methodology is provided that can prevent such phenomena and lead to the design of a suitable filter.

For further research and analysis it would be recommended to run simulations with the grid side of the model also included, to simulate grid fluctuations of voltage and frequency too. Furthermore, it would be beneficial to investigate the behaviour of a model with more than one tidal devices where several units (tidal generator along with subsea cable and converter) go through one transformer instead of separate ones in order to view how the parallel resonance changes. Another model configuration for studying parallel resonance phenomena could be to have several tidal generators connected to one frequency converter through subsea cables, although this configuration is not recommended for a tidal system, as mentioned before.

Additionally, a more detailed model in terms of inverter controls could be assessed. This would enable a sensitivity analysis from an electromagnetic compatibility and interference aspect, apart from the harmonic content investigation, as the different values of amplitude modulation index (m_a) and switching frequency (f_s) can have considerable influence at both conducted electromagnetic interference (EMI) and total harmonic distortion of the system (%THD) (Khamphakdi, et al., 2006).

Another suggestion would be to mask the system's parameters and run simulations through a script in order to gather results and compare them more easily.

6 Appendices

6.1 Appendix A

Code generation

Matlab code was generated as an attempt to run unattended simulations as well as gather and compare results from different runs. The script that is presented bellow opens a Simulink model, masks the requested parameters, then runs simulations for the different masked values and performs fft analysis which then plots the harmonic spectrum of each case.

```
open_system('file_name'); %opens simulink model
        for i=3:7
        set_param('file_name/Pi Secton Line','Length','i'); %masks
cable and sets different values for cable length
        set_param('file_name/Pi Secton Line1','Length','i');
        set_param('file_name/Pi Secton Line2','Length','i');
        end

        for i=47:52
        set_param('file_name/Asynchronous Machine SI
Units','NominalParameters','[1455e+03 6600 i]'); %masks generator and
sets fifferent values for frequency
        end

sim('file_name'); %command to start simulation from script
```

After running the simulations the following code receives the data structure fourier (as seen in figure 2.2), performs fourier analysis and plots the harmonic spectrum.

```matlab
%Receiving as input a time structure like the one called fourier
% -fourier.signals.values gives a matrix with 3 columns each of whom
gives
% the time series of voltage of each phase
%-fourier.time gives the time vector of the recorded voltage signal

%separating the phases & time
a=fourier.signals.values(:,1); %phase A
b=fourier.signals.values(:,2); %phase B
c=fourier.signals.values(:,3); %phase C
t=fourier.time;                %time vector



%creating time-series objects for each phase
ts1=timeseries(a,t);
ts2=timeseries(b,t);
ts3=timeseries(c,t);

%time window & resampling
fundf=49.2; %fundamental frequency
ncycles=10; %number of cycles to be sampled
t0=6.7;     %start time of sampling
fs=2^19;    %sampling frequency, 1/fs is the time distance between
sampled observations
tnew=linspace(t0,ncycles/fundf+t0,ncycles*fs/fundf+1); %creating new
time vector

%creating new time vectors for each phase
ts1new=resample(ts1,tnew,'linear');
ts2new=resample(ts2,tnew,'linear');
ts3new=resample(ts3,tnew,'linear');

%the ratio of fsactual to NFFT denotes the space between 2
concecutive frequencies.
%Therefore, nfft is set to 2^21 so that the space between two
frequencies
%is set at 0.5Hz and we can come as close to the funsamental
frequency as
%possible
nfft= 2^21;

% Takes fft for each phase, padding with zeros so that length(fftx)
is equal to nfft
mxa = fft(ts1new.data,nfft)/length(ts1new.data);
mxb = fft(ts2new.data,nfft)/length(ts2new.data) ;
mxc = fft(ts3new.data,nfft)/length(ts3new.data);

mxa=2*abs(mxa(1:nfft/2+1));
mxb=2*abs(mxb(1:nfft/2+1));
mxc=2*abs(mxc(1:nfft/2+1));
```

```matlab
%there is always a difference between the user defined frequency
increment
%and the actual frequency increment. This part calculated the actual
%frequency increment.
fsactual=1/(tnew(2)-tnew(1));
f = fsactual / 2 * linspace(0, 1, nfft/2+1);

%Find max amplitudes for each phase
relmxa=mxa/max(mxa);
relmxb=mxb/max(mxb);
relmxc=mxc/max(mxc);

% Generate the plot, title and labels for each phase
%make a new figure
%Phase A
figure;
bar(f,relmxa);
title('Harmonic Spectrum');
xlabel('Frequency (Hz)');
ylabel('% of fundamental f');
axis([0 6000 0 1]);%sets the axes ranges; x-axis is set according to
the
                   %maximum frequency that we want to investigate
                   %y-axis is set for the desired maximum magnitude
%Phase B
figure;
bar(f,relmxb);
title('Harmonic Spectrum');
xlabel('Frequency (Hz)');
ylabel('% of fundamental f');
axis([0 6000 0 1]);
%Phase C
figure;
bar(f,relmxc);
title('Harmonic Spectrum');
xlabel('Frequency (Hz)');
ylabel('% of fundamental f');
axis([0 6000 0 1]);
```

Figure 7.1 displays two Simulink blocks with masked parameters; that of the subsea cable where the length is masked and that of the generator where the frequency and the mutual inductance are masked as an example. It should be noted at this point that an accurate representation of a masked cable would require further investigation as this algorithm varies the cable length but not the number of PI sections.
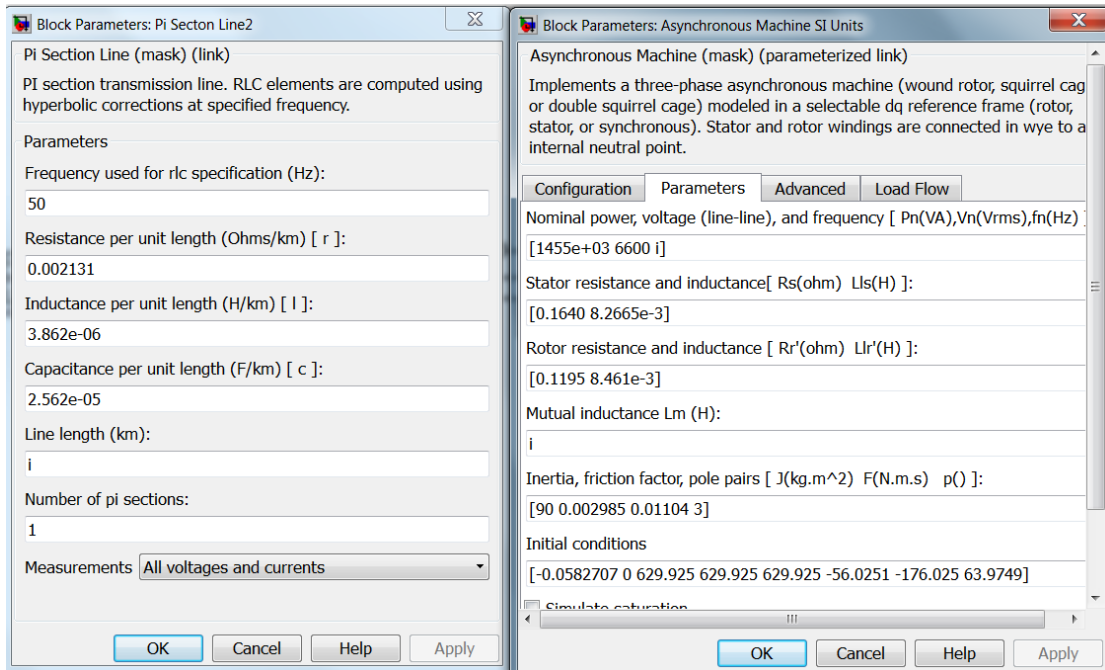
Figure 6.1Simulink masked block parameters

Just to give an insight on the code's deliverables figures 7.2 and 7.3 demonstrate the resulting plots of the matlab code for different plotting settings.
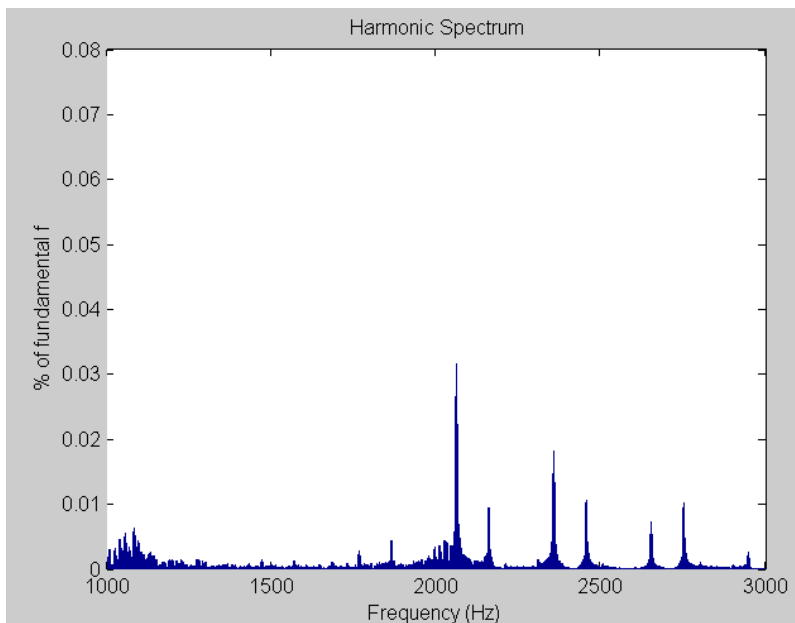
Figure 6.2Outcome of matlab code for max percentage of fundf=1
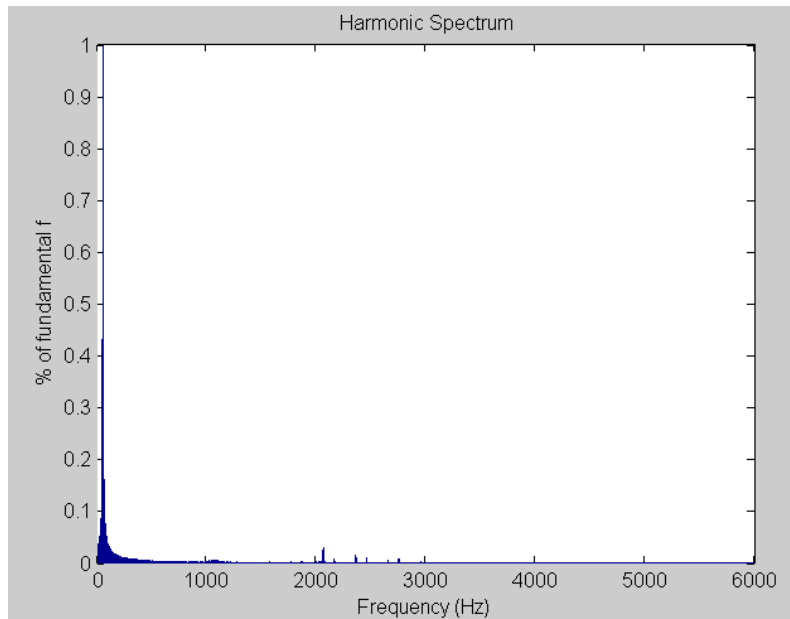
Figure 6.3Outcome of matlab code for max percentage of fundf=0.08

6.2   Appendix B

In this section the results of the simulation results are provided in detail in the form of excel sheets.

Table 6-1Simulations with varying cable length

		%THD					
PI sections	overall length	Vgen1	Vgen2	vgen3	Vgt1	Vgt2	Vgt3
2	3	2.05	2.24	2.20	1.91	2.10	2.06
3	3.5	1.27	1.27	1.49	1.23	1.22	1.47
3	4	1.27	1.27	1.49	1.23	1.22	1.47
3	4.5	1.27	1.27	1.49	1.23	1.22	1.47
3	5	1.27	1.27	1.49	1.23	1.22	1.47
4	5.5	1.52	1.40	1.26	1.51	1.38	1.22
4	6	1.52	1.40	1.26	1.51	1.38	1.22
4	6.5	1.52	1.40	1.26	1.51	1.38	1.22
4	7	1.52	1.40	1.26	1.51	1.38	1.22
5	7.5	1.25	1.47	1.46	1.24	1.48	1.46
5	8	1.25	1.47	1.46	1.24	1.48	1.46
5	8.5	1.25	1.47	1.46	1.24	1.48	1.46
5	9	1.25	1.47	1.46	1.24	1.48	1.46
6	9.5	1.35	1.91	1.57	1.35	1.95	1.59
6	10	1.35	1.91	1.57	1.35	1.95	1.59

Table 6-2Results for varying magnetising inductance in the transformer

Inductance	%THD					
H	Vgen1	Vgen2	vgen3	Vgt1	Vgt2	Vgt3
3.00E-06	1.33	1.45	1.42	1.22	1.37	1.34
5.00E-06	1.49	1.57	1.61	1.33	1.43	1.47
1.00E-05	1.89	2	1.93	1.67	1.8	1.72
3.00E-05	6.21	6.28	6.36	5.29	5.36	5.42
5.00E-05	32.72	32.5	32.8	29.27	29.08	29.35
6.00E-05	14.12	14.23	14.17	12.79	12.89	12.84
7.00E-05	1.97	2.13	2.07	1.8	1.97	1.9
1.00E-04	1.29	1.43	1.41	1.21	1.4	1.35
1.10E-04	1.08	1.3	1.24	1.03	1.29	1.22
1.20E-04	0.98	1.2	1.13	0.95	1.21	1.13
1.30E-04	0.98	1.55	1.29	0.96	1.54	1.28
1.40E-04	0.89	1.26	1.17	0.89	1.27	1.18
2.00E-04	0.96	1.22	1.26	0.97	1.24	1.27
2.40E-04	0.94	1.24	1.24	0.95	1.26	1.26
2.70E-04	1.18	1.16	1.09	1.19	1.18	1.11
3.00E-04	0.97	1.1	0.98	0.98	1.12	1.01
4.00E-04	0.94	1.36	1.13	0.96	1.39	1.16
5.00E-04	0.99	1.33	1.15	1.02	1.37	1.18
6.00E+00	0.85	1.21	1.09	0.88	1.25	1.12
1.00E-03	1.58	1.58	0.96	1.62	1.63	0.99
1.30E-03	7.43	6.14	6.92	7.03	5.83	5.98
1.50E-03	9.65	11.42	8.05	9.13	10.81	7.64
1.60E-03	8.36	8.88	6.29	7.92	8.43	5.99
1.70E-03	16.21	21.57	15.85	15.34	20.4	15
1.80E-03	10.45	8.78	10.23	9.89	8.33	9.69
1.90E-03	29.83	23.98	28.64	28.21	22.68	27.09
2.00E-03	36.14	26.97	43.5	34.19	25.53	41.16
2.10E-03	32.08	26.3	37.27	30.36	24.89	35.28

Table 6-3 Results for varying inductance in the output reactor

inductor			%THD			
µH	Vgen1	Vgen2	vgen3	Vgt1	Vgt2	Vgt3
90	1.29	1.43	1.41	1.21	1.4	1.35
80	1.41	1.68	1.64	1.31	1.62	1.58
70	1.69	1.84	1.79	1.57	1.76	1.68
60	2.09	2.23	2.2	1.92	2.1	2.05
50	2.63	3.01	2.89	2.41	2.83	2.68
40	3.24	3.61	3.46	3.08	3.44	3.31
100	1.19	1.23	1.3	1.13	1.2	1.26
110	1.2	1.14	1.35	1.17	1.12	1.34
120	1.06	1.02	1.16	1.04	1.01	1.15

Table 6-4 Results for filter tuned at low order harmonics

				Filter Tuned for low order harmonics							
order	f	ω	C	L		%THD					
	Hz	rad/sec	F	H	Vgen1	Vgen2	vgen3	Vgt1	Vgt2	Vgt3
5	250	1570	0.000381	0.001064	5.31	5.3	5.32	4.58	4.58	4.6
7	350	2198	0.000272	0.00076	5.27	5.33	5.29	4.95	5	4.97
11	550	3454	0.000173	0.000484	4.89	4.97	4.93	4.38	4.47	4.43
13	650	4082	0.000147	0.000409	4.95	5.04	5.01	4.45	4.54	4.52
15	750	4710	0.000127	0.000355	5.04	5.11	5.08	4.49	4.57	4.54
17	850	5338	0.000112	0.000313	5.11	5.18	5.14	4.57	4.66	4.62
18	900	5652	0.000106	0.000296	5.15	5.23	5.18	4.61	4.71	4.66
19	950	5966	0.0001	0.00028	5.25	5.37	5.29	4.71	4.84	4.76
20	1000	6280	9.53E-05	0.000266	5.28	5.31	5.29	4.73	4.77	4.75
21	1050	6594	9.08E-05	0.000253	5.3	5.36	5.32	4.75	4.81	4.78
22	1100	6908	8.67E-05	0.000242	5.33	5.4	5.36	4.77	4.86	4.81
23	1150	7222	8.29E-05	0.000231	5.39	5.45	5.42	4.83	4.9	4.86
24	1200	7536	7.94E-05	0.000222	5.45	5.5	5.47	4.89	4.94	4.91
25	1250	7850	7.63E-05	0.000213	5.54	5.59	5.55	4.98	5.04	5

Table 6-5 Results for filter tuned at high order harmonics

				Filter Tuned for high order harmonics							
order	f	ω	C	L					%THD		
	Hz	rad/sec	F	H		Vgen1	Vgen2	vgen3	Vgt1	Vgt2	Vgt3
40	2000	12560	4.77E-05	0.000133		4.53	4.56	4.55	4.03	4.07	4.07
41	2050	12874	4.65E-05	0.00013		4.22	4.26	4.26	3.75	3.8	3.8
42	2100	13188	4.54E-05	0.000127		3.93	4.01	4.02	3.49	3.59	3.59
43	2150	13502	4.43E-05	0.000124		3.59	3.67	3.68	3.17	3.27	3.28
46	2300	14444	4.14E-05	0.000116		2.65	2.75	2.76	2.33	2.47	2.46
47	2350	14758	4.06E-05	0.000113		2.31	2.47	2.45	2.04	2.24	2.2
48	2400	15072	3.97E-05	0.000111		2.13	2.29	2.24	1.91	2.11	2.04
49	2450	15386	3.89E-05	0.000109		2.01	2.17	2.12	1.83	2.03	1.96
50	2500	15700	3.81E-05	0.000106		1.87	2.05	1.98	1.73	1.95	1.86
51	2550	16014	3.74E-05	0.000104		1.79	1.99	1.92	1.67	1.9	1.81
52	2600	16328	3.67E-05	0.000102		1.78	1.98	1.9	1.66	1.89	1.81
53	2650	16642	3.6E-05	0.0001		1.82	2.02	1.94	1.7	1.93	1.84
54	2700	16956	3.53E-05	9.85E-05		1.89	2.08	2.01	1.76	1.98	1.9
55	2750	17270	3.47E-05	9.67E-05		1.98	2.17	2.1	1.84	2.05	1.97
56	2800	17584	3.4E-05	9.5E-05		2.09	2.27	2.2	1.93	2.14	2.05
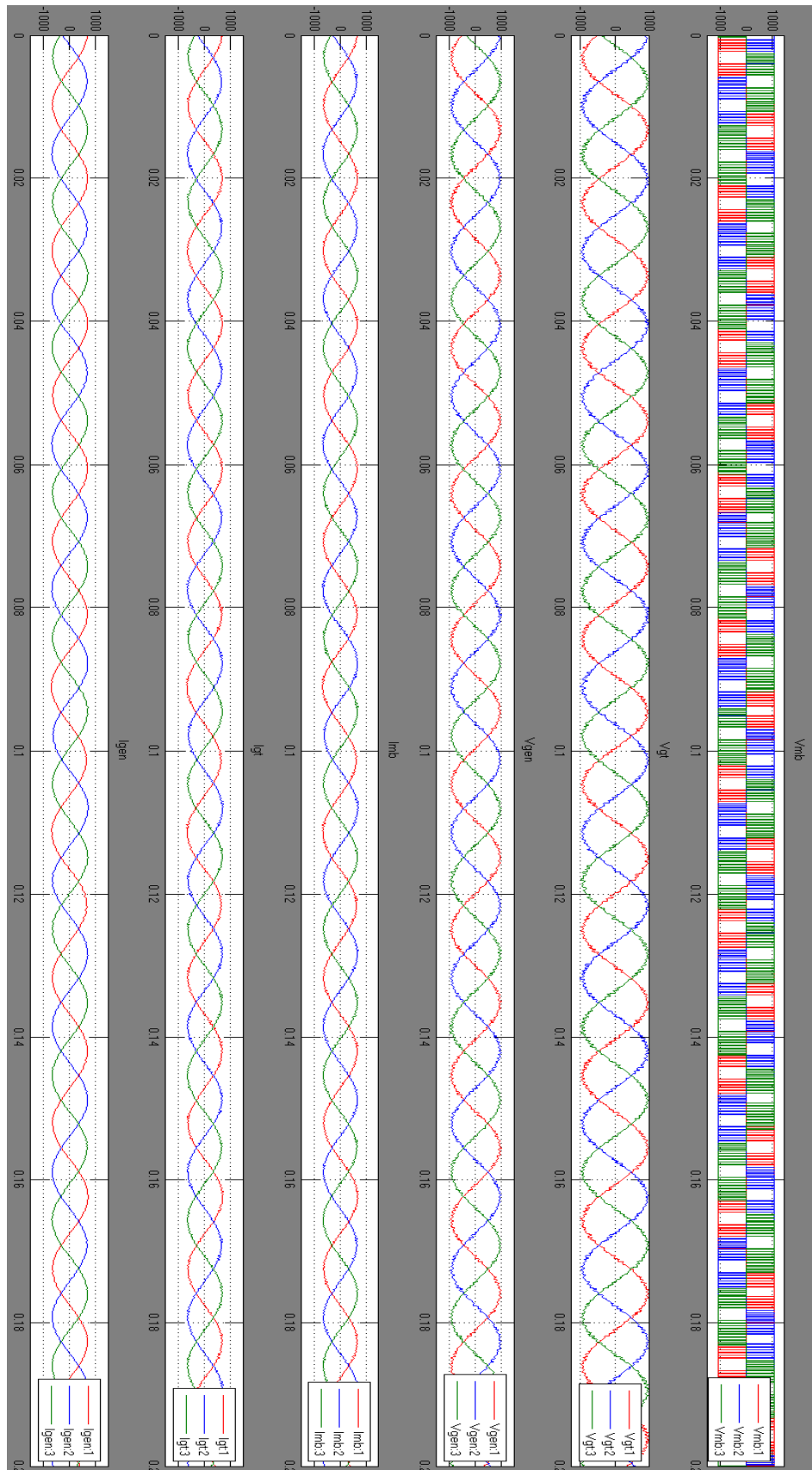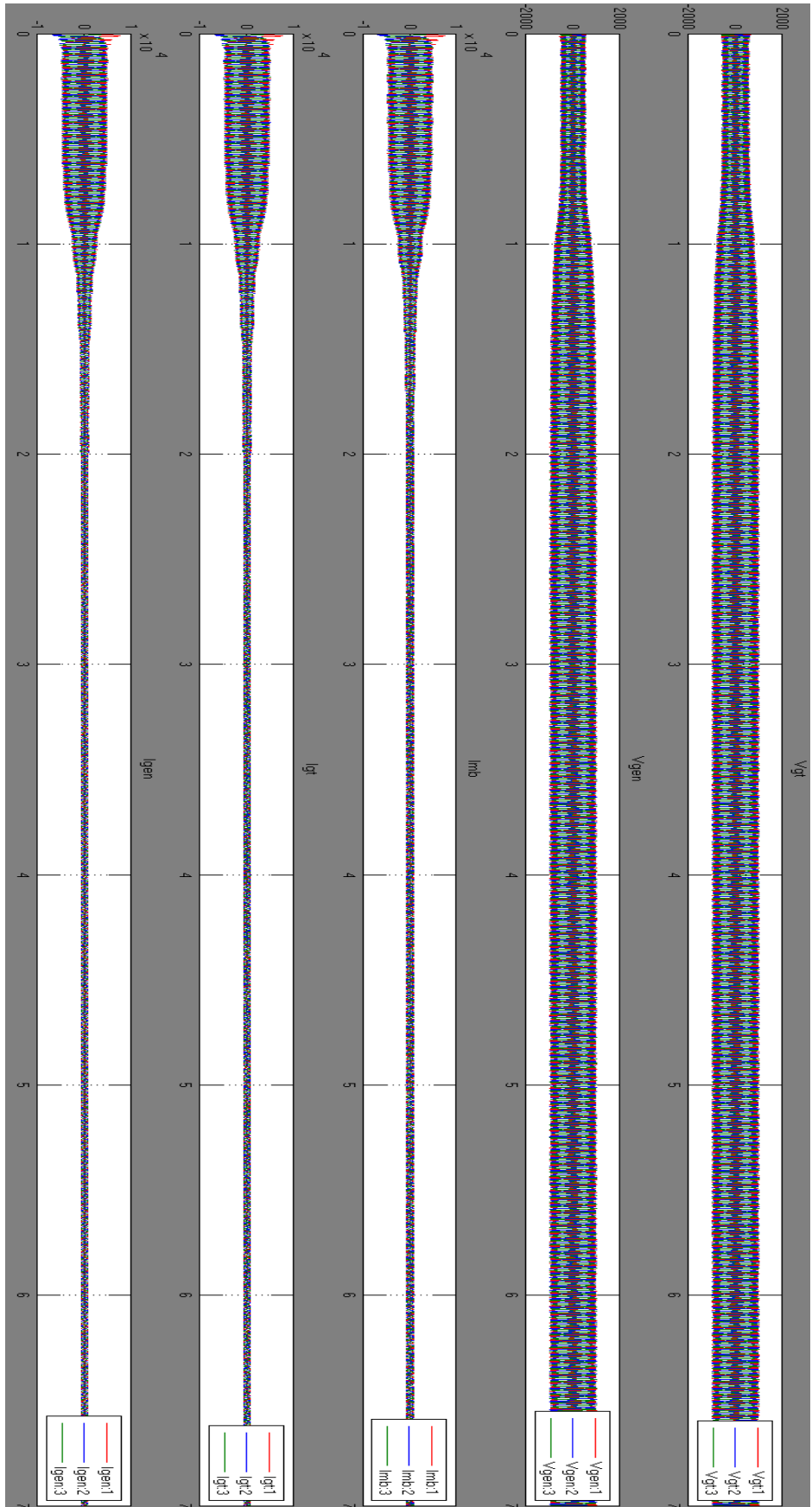
7 Bibliography

Acha, E., Agelidis, V. G., Anaya-Lara, O. & Miller, T., 2002. *Power Electronic Control in Electrical Systems.* 1st ed. s.l.:Newnes.

Amin, A. M. A., 1997. Line Current Harmonic Reduction in Adjustable-Speed Induction Motor Drive by Harmonic Current Injection. *IEEE, Industrial Electronics*, pp. 312-317.

Anaya-Lara, O. et al., 2009. *Wind Energy Generation Modelling and Control.* 1st ed. s.l.:John Wiley & Sons, Ltd..

Arrillaga, J. & watson, N. R., 2003. *Power System Harmonics.* 1st ed. s.l.:John Wiley & Sons.

B.P.Conroy, Summer, M. & Alexander, T., 1995. Application of Encoderless Vector Control Techniques in a Medium Performance Induction Motor Drive. *IEEE, IET Conference Publications*.

Blunden, L. & Bahaj, A. S., 2006. Initial evaluation of tidal stream energy resources at Portland Bill, UK. *Renewable Energy,* 31(6), pp. 121-132.

Böhmeke, G., Boldt , R. & Beneke, H., 1997. *Geared drive intermediate solutions, comparisons of design features and operating economics.* s.l., Proc. 1997 Europ. Wind Energy Conf..

Bose, B. K., 2006. *Power Electronics and Motor Drives : Advances and Trends.* London: Academic Press.

Bose, B. & van Wyk, J., 1997. Power Electronic Converters for Drives (Chapter 3). In: *Power Electronic Converters for Variable Frequency Drives.* s.l.:Wiley-IEEE Press, pp. 80 -137.

Chapman, S. J., 2000. *Electric Machinery Fundamentals.* 3rd ed. s.l.:McGraw-Hill.

Charlier, R., 2003. A 'sleeper' awakes: tidal current power.. *Renewable and Sustainable Energy Reviews,* 7(6), pp. 515-529.

Cnes, 2000. *AVISO.* [Online]
Available at: http://www.aviso.oceanobs.com/en/news/idm/2000/oct-2000-sun-and-moon-shape-tides-on-earth/index.html
[Accessed 7 June 2012].

Daniel J. Carnovale, P., Thomas, D. J. & Blooming, T. M., 2003. *Price and Performance Consideration for Harmonic Solutions.* Chicago, s.n.

EMEC, 2012. *EMEC Orkney.* [Online]
Available at: http://www.emec.org.uk/marine-energy/
[Accessed 20 August 2012].

Fitzgerald, A., Kingsley, C. J. & Umans, S. D., 2003. *Electric Machinery.* 6th ed. s.l.:McGraw-Hill.

Harmonic Media, 2012. *Electrical Design Tutor.* [Online]
Available at: http://www.electrical-design-tutor.com/squirrelcagemotors.html
[Accessed 8 June 2012].

IEEE STANDARDS, 1993. IEEE Recommended Practices and Requirements for Harmonic Control in Electrical Power Systems. 2 April.

Jones, R. & Smith, G. A., 1993. High Quality Mains Power From Variable-Speed Wind Turbines. *IEEE, IET Conference Publications,* Volume 385, pp. 202-206.

Khamphakdi, P., Tarateeraseth, V., Karanun, K. & Khan-ngern, W., 2006. *The Conducted Electromagnetic Interference of Small Grid Connected Inverter to Power System.* Zurich, 17th International Zurich Symposium on Electromagnetic Compatibility.

Liang, X. & Jackson, W., 2008. Influence of Subsea Cables on Offshore Power Distribution Systems. *IEEE, Transactions on Industry Applications.*

McLean, A., McLeay, K. & Sheldrake, A., 1993. *Harmonic Suppression Filter for Offshore Interconnected Power System.* London, IEE.

Mohan, N., Underland, T. M. & Robbins, W. P., 1995. *POWER ELECTRONICS Converters, Applications and Design.* 2nd ed. s.l.:John Wiley & Sons, Inc..

Oppenheim, A. V., 1987. *Signals ans Systems.* 1st ed. Boston, Massachussets: MIT Center for Advanced Engineering Study.

RH., C., 2003. A 'sleeper' awakes: tidal current power.. *Renewable and Sustainable Energy Reviews,* 7(6), pp. 519-529.

Rosa, F. C. D. l., 2006. *Harmonics and Power Systems.* s.l.:Taylor & Francis Group.
Sandoval, G. & Houdek, J., 2005. A Review of Harmonic Mitigation Techniques.

Sheth, S. & Shahidehpour, M., 2005. Tidal Energy in Electric Power Systems. *IEEE, Conference Publications.*

Strathclyde, E.-U. o., 2005. *Tidal Principles.* [Online]
Available at: http://www.esru.strath.ac.uk/EandE/Web_sites/03-04/marine/res_resourcebkd.htm
[Accessed June 2012].

Thede, L., 2004. *Practical Analog and Digital Filter Design.* s.l.:Artech House, Inc..

VanderMeulen, A. & Maurin, J., 2010. Current Source Inverter vs. Voltage Source Inverter Topology. *EATON.*

Winder, S., 2002. *Analog and Digital Filter Design.* s.l.:Elsevier Gulf.

Wu, B., 2006. *High Power Converters and AC Drives.* s.l.:IEEE press, Jon Willey & Sons Inc..

Yazdani, A. & Iravani, R., 2010. *Voltage-Sourced Converters in Power Systems: Modeling, Control and Applications.* New Jersey: John Wiley & Sons Inc..

Zaimeddine, R. & Undeland, T., 2010. Direct Torque Control Scheme For Dual-Three-Phase Induction Motor. *IEEE Conference Publications,* pp. 3007-3014.